

Wilfrid Laurier University

Scholars Commons @ Laurier


Theses and Dissertations (Comprehensive)

2010

Microporous Organic Polymers: Synthesis and Post Synthetic Modifications

Phillip Andrew Kerneghan
Wilfrid Laurier University

Follow this and additional works at: <https://scholars.wlu.ca/etd>

 Part of the [Organic Chemistry Commons](#), and the [Polymer Chemistry Commons](#)

Recommended Citation

Kerneghan, Phillip Andrew, "Microporous Organic Polymers: Synthesis and Post Synthetic Modifications" (2010). *Theses and Dissertations (Comprehensive)*. 985.
<https://scholars.wlu.ca/etd/985>

This Thesis is brought to you for free and open access by Scholars Commons @ Laurier. It has been accepted for inclusion in Theses and Dissertations (Comprehensive) by an authorized administrator of Scholars Commons @ Laurier. For more information, please contact scholarscommons@wlu.ca.



Library and Archives
Canada

Published Heritage
Branch

395 Wellington Street
Ottawa ON K1A 0N4
Canada

Bibliothèque et
Archives Canada

Direction du
Patrimoine de l'édition

395, rue Wellington
Ottawa ON K1A 0N4
Canada

Your file *Votre référence*
ISBN: 978-0-494-68713-0
Our file *Notre référence*
ISBN: 978-0-494-68713-0

NOTICE:

The author has granted a non-exclusive license allowing Library and Archives Canada to reproduce, publish, archive, preserve, conserve, communicate to the public by telecommunication or on the Internet, loan, distribute and sell theses worldwide, for commercial or non-commercial purposes, in microform, paper, electronic and/or any other formats.

The author retains copyright ownership and moral rights in this thesis. Neither the thesis nor substantial extracts from it may be printed or otherwise reproduced without the author's permission.

AVIS:

L'auteur a accordé une licence non exclusive permettant à la Bibliothèque et Archives Canada de reproduire, publier, archiver, sauvegarder, conserver, transmettre au public par télécommunication ou par l'Internet, prêter, distribuer et vendre des thèses partout dans le monde, à des fins commerciales ou autres, sur support microforme, papier, électronique et/ou autres formats.

L'auteur conserve la propriété du droit d'auteur et des droits moraux qui protègent cette thèse. Ni la thèse ni des extraits substantiels de celle-ci ne doivent être imprimés ou autrement reproduits sans son autorisation.

In compliance with the Canadian Privacy Act some supporting forms may have been removed from this thesis.

While these forms may be included in the document page count, their removal does not represent any loss of content from the thesis.

Conformément à la loi canadienne sur la protection de la vie privée, quelques formulaires secondaires ont été enlevés de cette thèse.

Bien que ces formulaires aient inclus dans la pagination, il n'y aura aucun contenu manquant.


Canada

Microporous Organic Polymers: Synthesis and Post Synthetic Modifications

By

Phillip Andrew Kerneghan

BBSc, Wilfrid Laurier University, 2008

THESIS

presented to The Faculty of Science, Department of Chemistry

in partial fulfillment of the

requirements for the degree of

Master of Science

in

Chemistry

Wilfrid Laurier University

2010

© Phillip Andrew Kerneghan 2010

AUTHOR'S DECLARATION

I hereby declare that I am the sole author of this thesis. This is a true copy of the thesis, including any required final revisions, as accepted by my examiners.

I understand that my thesis may be made electronically available to the public.

Phil Kerneghan

Abstract

Microporous solids are an important class of materials that have been studied extensively. Newer to this field are Microporous Organic Polymers (MOPs) which are networks constructed from smaller organic building blocks and exhibit large surface areas, small pore sizes and low densities. It is due to these characteristics that MOPs have attracted attention because of their potential use in applications such as catalysis, chemical separations and gas storage.

In this thesis is described the synthesis of two novel MOPs, the first of which being a network based on benzenediboronic acid and triptycene building blocks linked together by boronate esters. This network showed a relatively low surface area of $200 \text{ m}^2\text{g}^{-1}$ and guest uptake capacities of 18 % by mass. However, this network proved to be chemically unstable and the boronate ester linkages degrading when exposed to air. The second network was formed via Yamamoto coupling conditions and was based on tetraphenylbimesityl monomers. This network also showed a guest solvent uptake capacity of 18 % by mass while maintaining thermal stability up to $400 \text{ }^\circ\text{C}$. The network also showed a relatively large surface area of $1424 \text{ m}^2\text{g}^{-1}$.

In addition to synthesizing novel frameworks it was also possible to post synthetically modify two additional networks. The first post synthetic modifications to a purely organic microporous material were performed on a network originally linked by imine bonds. First, the imine bonds within the network were reduced to amine bonds resulting in the network becoming more resistant to hydrolysis. However, because the rigid imine bonds were reduced, the network was allowed to collapse and permanent

microporosity was lost. The amine bonds within the network were then acetylated in order to demonstrate that further post synthetic modifications were possible.

The second network that we performed post synthetic modifications on was a Porous Aromatic Framework (PAF) comprised of tetraphenylmethane monomers. This network was brominated via electrophilic aromatic substitution to the phenyl rings present within the network. Modifications to this network resulted in a decrease in surface area from $2250 \text{ m}^2\text{g}^{-1}$ to $694 \text{ m}^2\text{g}^{-1}$ and solvent guest uptake capacity from 28 % by mass to 16 % by mass.

Acknowledgements

I would first like to thank my mom, Maribeth, and dad, David, for all of their never ending love and support, financial included. Mom, thank you for all of your fantastic guidance and weekly phone conversations that often kept me on track. I couldn't have done it without your support. Dad, thanks for coming home everyday and telling me "Phillip, don't ever be an accountant!" I'm sure he's watching and approves of chemistry.

I would also like to extend a special thank you to my supervisor Ken Maly for taking me in as his first Masters student. I especially appreciate your humour, kindness and friendship that made my time as an MSc student very enjoyable. I couldn't have survived with any supervisor other than you. I would also like to thank all of the peers whom I worked with in Ken's lab: Lynett, Shira, Marc, Andrew, Melissa, Caitlin, Katie, Tyler, Colin, Josh and Joe. We definitely had a lot of fun and made work never seem like work. Thank you to Professor David Bryce from the University of Ottawa for all of your assistance in running solid state NMR's for me and thank you to Dr's John Ripmiester and Steven Lang for inviting me to the NRC-SIMS and teaching me about gas adsorption.

Funding for this thesis was provided NSERC and Wilfrid Laurier University.

Table of Contents

AUTHOR'S DECLARATION	i
Abstract	ii
Acknowledgements	iv
Table of Contents	v
List of Figures	vi
List of Schemes	viii
Abbreviations	ix
Chapter 1: Introduction	1
1.1 Microporous Materials.....	1
1.2 Metal Organic Frameworks	3
1.3 Polymers of Intrinsic Microporosity	5
1.4 Microporous Organic Polymers	7
1.5 Post Synthetic Modifications of Microporous Materials	11
1.6 Research Objectives.....	13
Chapter 2: Novel Triptycene Based Framework	15
2.1 Introduction.....	15
2.2 Synthesis	18
2.3 Results and Discussion	21
2.4 Summary	25
Chapter 3: Post Synthetic Modifications to an Imine Linked MOP.....	26
3.1 Introduction.....	26
3.2 Model Studies	27
3.3 Synthesis	29
3.4 Characterization of Networks	31
3.5 Summary.....	41
Chapter 4: Synthesis and PSM to Porous Aromatic Frameworks (PAFs)	42
4.1 Introduction of Tetraphenylmethane based PAFs.....	42
4.2 Synthesis and Characterization of Tetraphenylmethane based PAFs	43
4.2 Discussion of Tetraphenylmethane based PAFs.....	48
4.3 Bimesityl PAF Introduction.....	50
4.4 Synthesis of Bimesityl PAF	50
4.5 Characterization of Bimesityl PAF	52
4.6 Summary	55
Chapter 5: Conclusions and Future Work	56
Chapter 6: Experimental	58
6.1 General.....	58
6.1.1 <i>Infrared Spectroscopy</i>	58
6.1.2 <i>NMR Spectroscopy</i>	58
6.1.3 <i>Elemental Analysis</i>	58
6.1.4 <i>Carbon-13 CP/MAS NMR spectroscopy</i>	58
6.1.5 <i>Gas Adsorption Studies</i>	59
6.1.6 <i>Thermogravimetric Analysis</i>	60
6.2 Synthesis	60
Chapter 7: References	75

List of Figures

Figure 1-1: General schematic showing the linking of polytopic building blocks to form synthetic networks.....	2
Figure 1-2a: Representative formation of a Metal Organic Framework.....	4
Figure 1-2b: Crystal structure of MOF-5.....	4
Figure 1-3: A general scheme illustrating the concept of post synthetic modifications to a porous framework.....	12
Figure 1-4: Scheme of representative post synthetic modification to IRMOF-3 with various anhydrides.....	12
Figure 2-1: IR spectrum of model compound 5.....	20
Figure 2-2: IR spectrum of Triptycene MOP.....	22
Figure 2-3: Nitrogen isotherm plot of Triptycene MOP.....	23
Figure 2-4: Thermogravimetric analysis of Triptycene MOP.....	24
Figure 3-1: Infrared spectra of model compounds.....	28
Figure 3-2: Infrared spectra of Imine MOP, Reduced MOP, Amide MOP.....	32
Figure 3-3: ^{13}C CP-MAS spectra of Imine MOP, Reduced MOP, Amide MOP.....	33
Figure 3-4: TGA traces of Imine MOP with THF, activated, and resolvated with THF.....	34
Figure 3-5: Nitrogen adsorption isotherm for Imine MOP and Reduced MOP.....	35
Figure 3-6: TGA traces of Reduced MOP with THF, activated, and resolvated with THF.....	37
Figure 3-7: Infrared spectrum of Reduced MOP after being subjected to aqueous acidic conditions.....	38

Figure 3-8: Nitrogen adsorption isotherm for Amide MOP.....	40
Figure 3-9: TGA traces of Amide MOP with THF, activated and resolvated with THF (green line).....	40
Figure 4-1: IR spectra of Tetraphenylmethane PAF and 12.....	45
Figure 4-2: Nitrogen gas adsorption isotherm of Tetraphenylmethane PAF Brominated PAF.....	46
Figure 4-3: IR spectra of Tetraphenylmethane PAF and Brominated PAF.....	48
Figure 4-4: TGA trace of Tetra(phenyl)methane PAF activated/THF guest and Brominated PAF activated/THF guest.....	49
Figure 4-5: IR spectra 15 and Bimesityl PAF.....	53
Figure 4-6: Nitrogen gas adsorption isotherm for Bimesityl PAF.....	54
Figure 4-7: TGA trace of Bimesityl PAF activated and THF guest.....	55

List of Schemes

Scheme 1-1: Synthesis of triptycene based PIM (Trip-PIM).....	6
Scheme 1-2: Boronate ester and boroxine linked COFs.....	8
Scheme 1-3: Imine linked MOP.....	9
Scheme 1-4: Yamamoto coupling formation of a Porous Aromatic Framework (PAF)....	9
Scheme 2-1: Synthesis of Triptycene MOP.....	18
Scheme 2-2: Synthesis of triptycene model compound 5.....	20
Scheme 3-1: Model reactions.....	27
Scheme 3-2: Synthesis of tetrakis(4-aminophenyl)methane building block 11.....	29
Scheme 3-3: Synthesis of Imine MOP.....	30
Scheme 3-4: Reduction and acetylation of Imine MOP.....	30
Scheme 4-1: General representation of a Yamamoto coupling.....	42
Scheme 4-2: Synthesis of Tetraphenylmethane PAF.....	43
Scheme 4-3: Bromination of Tetraphenylmethane PAF.....	47
Scheme 4-4: Synthesis of Bimesityl PAF.....	51

Abbreviations

BDBA	1,4-benzenediboronic acid
BET	Brunauer-Emmett-Teller
δ	chemical shift
CDCl_3	deuterated chloroform
COF	covalent organic framework
CP/MAS	cross polarization / magic angle apinning
DMF	dimethylformamide
DMSO	dimethyl sulphoxide
IR	infrared
M	molar
mmol	millimole
mol	mole
MOF	metal organic framework
MOP	microporous organic polymer
NMR	nuclear magnetic resonance
PAF	porous aromatic framework
PIM	polymer of intrinsic microporosity
TGA	thermogravimetric analysis
THF	tetrahydrofuran

Chapter 1: Introduction

1.1 Microporous Materials

Porous materials are networks of solid material which contain void spaces. These materials can be further classified depending on the size of the pores present in the material. Microporous solids are materials that contain permanent cavities with diameters of less than 2 nm. Mesoporous materials contain pores ranging from 2 nm to 50 nm and macroporous materials contain pores of greater than 50 nm.¹

The field of microporous materials contains several classes which are well known,² including naturally occurring zeolites, activated carbons and silica. Synthetic microporous solids have recently emerged as a potentially important class of materials. These include Metal Organic Frameworks (MOFs), Microporous Organic Polymers (MOPs) including Covalent Organic Frameworks (COFs) and Polymers of Intrinsic Microporosity (PIMs).³ It is the very large surface areas and very small pore sizes of these materials which make them of specific interest. These two factors permit microporous materials to be useful in applications such as heterogeneous catalysis, separation chemistry, and potential uses in hydrogen or other gas storage.^{4,5}

Most synthetic strategies to prepare microporous materials consist of linking together smaller units with ditopic or polytopic functionalities in order to form extended networks much like is displayed in the general diagram of Figure 1-1.

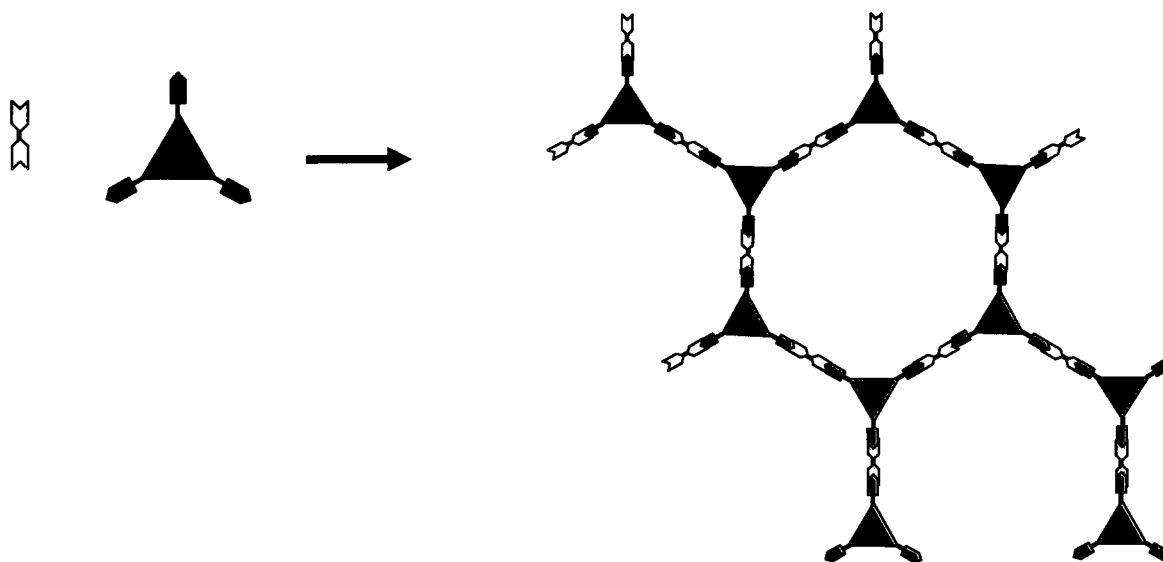


Figure 1-1: General schematic showing the linking of polytopic building blocks to form synthetic networks.

Whether a network formed is crystalline or amorphous is generally governed by whether the covalent bonds being formed involve reversible chemistry or not. Crystalline networks are typically formed under reversible reaction conditions that allow error corrections during network formation and produce thermodynamically stable networks. These types of reactions are commonly condensation reactions.⁶⁻⁸ On the other hand, when irreversible reactions are employed such as cross couplings, the networks tend to form in a disordered manner,^{9,10} resulting in amorphous materials. This is because a carbon-carbon bond is formed irreversibly under conditions such as a Sonagashira or Yamamoto couplings resulting in amorphous networks. This is of course unless some other templating measure is taking into account while considering the reaction conditions.¹¹

Certain factors such as temperature, solvent and solvent-to-head-space ratio, play an important role in the formation of a crystalline framework.⁶⁻⁸ Certain solvents can be employed in order to form ordered networks by means of their ability to dissolve the monomer building blocks. If the concentration of a monomer in solution is controlled by a solvent in which it is slightly soluble, then a network is more likely to form under thermodynamic, instead of kinetic control.^{9,10} Solvents could also be used based on their molecular size to act as templates for pores to form around.¹¹ While this idea of MOP/COF templating is generally understood in qualitative terms (i.e. which solvents produce crystalline networks) there has been no research into the quantitative effects (what solvent ratio is required to produce a well structured network).¹²

Finally, if a material is to exhibit microporosity, it must be composed of somewhat rigid building blocks in order to impart rigidity within the network and provide directionality for the formation of the network. This rigidity prevents collapse of the network upon itself and results in free volume which becomes the pores within a framework.

1.2 Metal Organic Frameworks

Porous coordination polymers were first pioneered by Robson who described the linking of $Zn(CN)_2$ and $Cd(CN)_2$ to rod-like connecting units such as 4,4'-bipyridine.¹³ These 3D frameworks, contain large pores which extend into channels throughout the network. Yaghi and coworkers later used this concept and prepared microporous coordination polymers referred to as Metal Organic Frameworks (MOFs). He linked coordinative metal nodes together using ditopic ligands such as 4,4'-bipyridine¹⁴ and

dicarboxylates, ¹¹ much like Robson, in order to form rigid porous frameworks. Specifically MOF-5 is formed via a reaction between zinc nitrate and 1,4-benzenedicarboxylic acid in DMF under solvothermal conditions in order to form an extended network as shown in Figure 1-2.

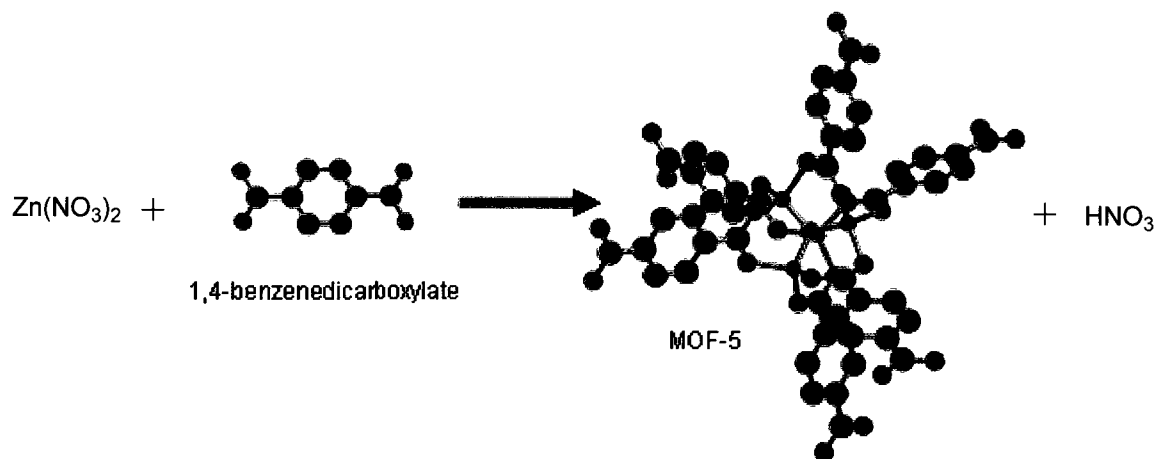


Figure 1-2a: Representative formation of a Metal Organic Framework

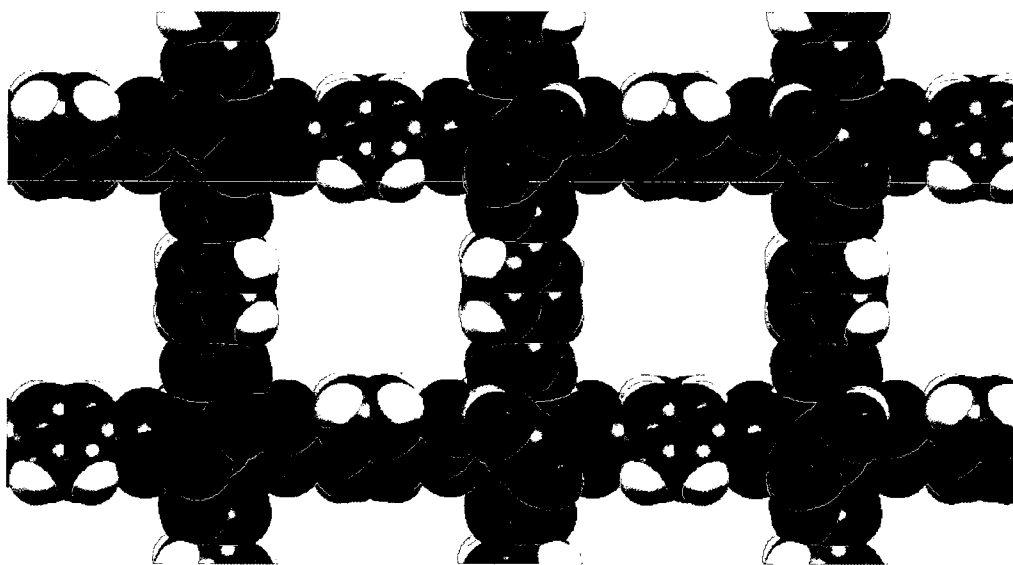


Figure 1-2b: Crystal structure of MOF-5.¹⁵

The network, once formed, shows distinct channels of 8 Å in diameter filled with DMF. The coordination bonds have also proven strong enough to withstand solvent exchange and even solvent evacuation while still maintaining the overall structure of the framework. Gas adsorption studies have also shown that the material has a surface area of 2900 m²g⁻¹.¹¹ Due to the attractive possible applications arising from the large surface areas and small pore sizes, the field of MOF chemistry has since expanded greatly to include many examples of networks formed by coordination complexes¹⁶ studied for their applications in hydrogen storage,^{17,18} chemical separation¹⁹ and catalysis.²⁰

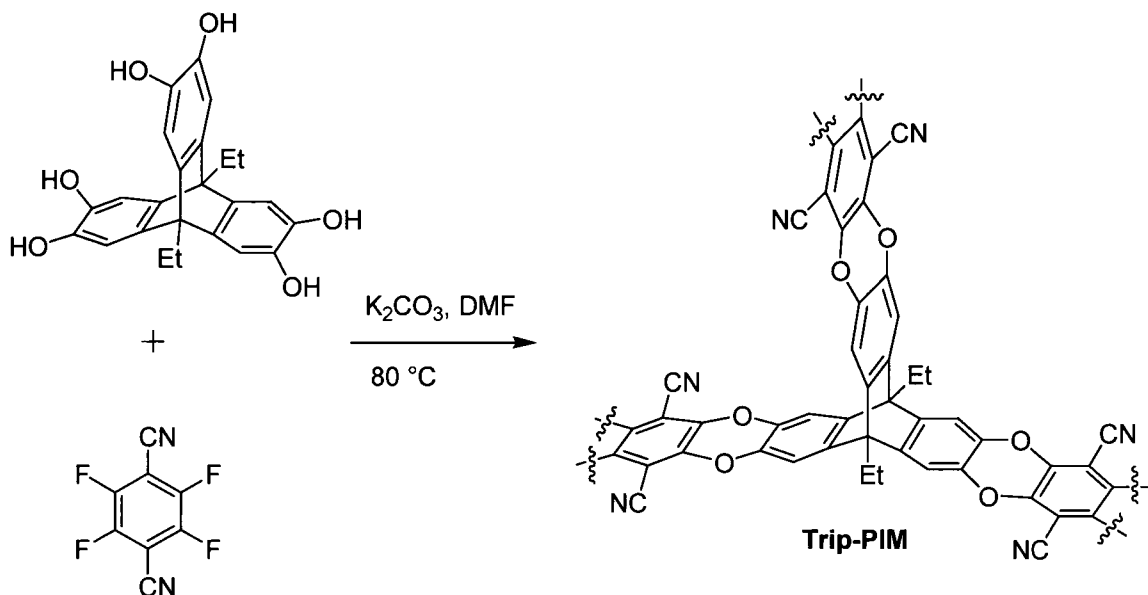
It is common however for MOF's to be very moisture sensitive at atmospheric pressures thus hindering their application as a gas storage media.²¹⁻²³ To combat this, the field has even been extended to MOF-carbon nanotube hybrids²⁴ which improve the stability of frameworks and have been studied for their hydrogen storage capacities.

1.3 Polymers of Intrinsic Microporosity

Purely organic microporous materials have been studied more recently and in far less depth compared to MOFs and other coordination polymers. Among the first examples of organic microporous materials were PIMs. Over the past decade, Budd, McKeown and coworkers have devised a new strategy for preparing microporous polymers which are able to maintain relatively high surface areas.²⁵⁻²⁹ By using bulky, rigid and nonlinear monomers, the resulting polymers are incapable of efficient packing and therefore results in micropores being formed between polymer layers. Over the past decade a variety of PIMs have been produced with surface areas ranging to over 1000

m^2g^{-1} . For example, a PIM derived from triptycene building blocks (Scheme 1-1) has a BET surface area of $1065 \text{ m}^2\text{g}^{-1}$.³⁰

Scheme 1-1: Synthesis of triptycene based PIM (**Trip-PIM**).³⁰



PIMs are formed in a kinetic manner using irreversible reaction conditions which presents one drawback of these systems. The resulting networks are amorphous and exhibit a broad pore size distributions making the materials less ideal for control and tuning of properties. However, regardless of lack of control over pore sizes, the high surface areas and pore volumes combined with functionality often present make PIMs a promising class of material for a range of applications where narrow pore size distributions are not required.

1.4 Microporous Organic Polymers

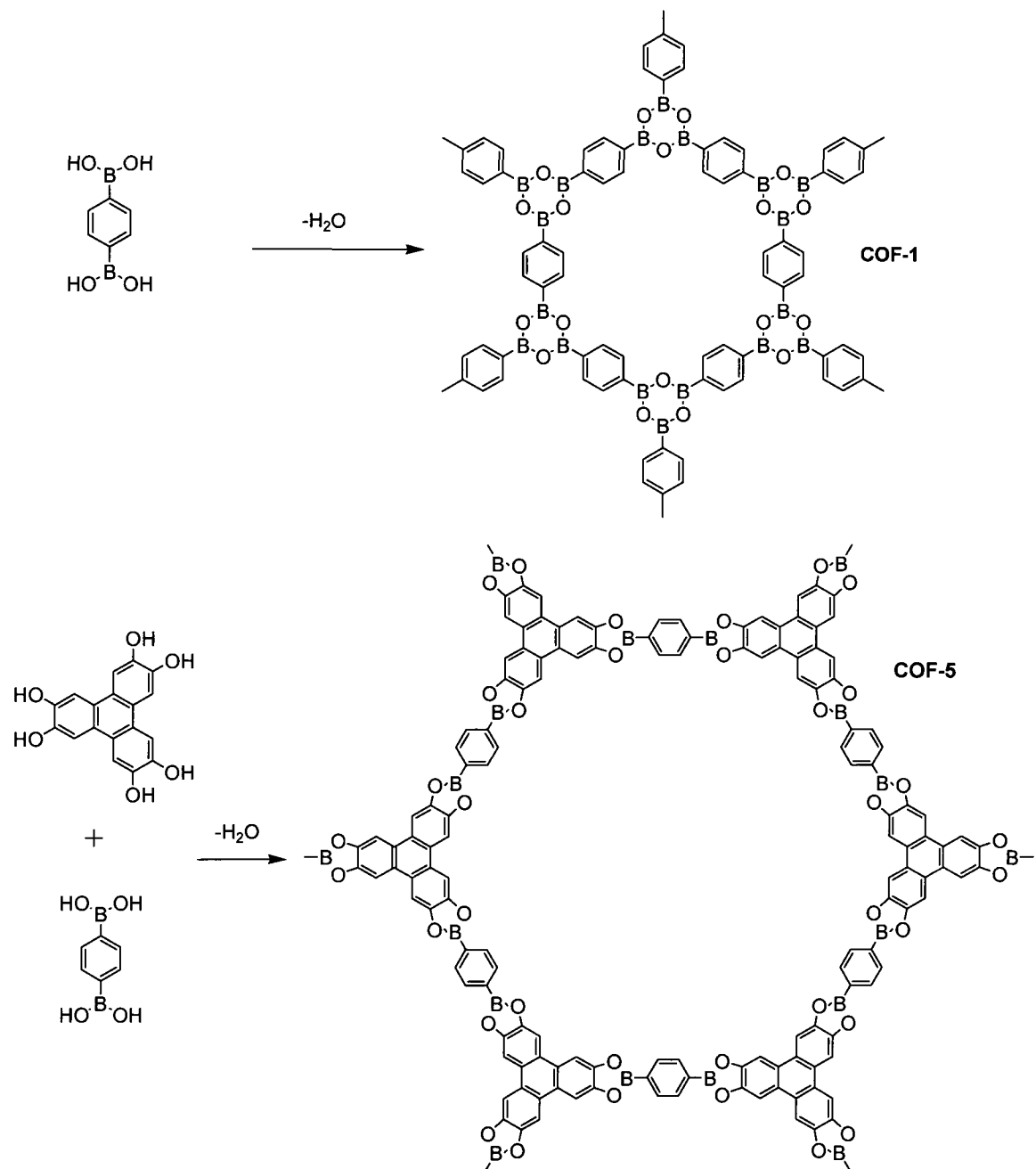
Many materials exhibit free volume such as organic polymers referred to as Polymers of Intrinsic Microporosity (PIMs),^{27,31} and of course MOFs.³²⁻³⁵ While the free space of PIMs arises from the rigid and awkward stacking of polymer layers upon themselves, the free space of MOFs is engineered in the synthesis, by using sturdy aromatic groups.¹² The same concept of engineering the free space based upon the rigidity of monomers used can be applied to the synthesis of MOPs.⁶⁻⁸

Also similar to MOFs, MOPs are generally formed by covalently linking organic molecular building blocks. MOPs can be broken into two broad classes consisting of ordered versus disordered materials.¹² Disordered amorphous networks are referred to as MOPs, however, if the networks are ordered and crystalline they are referred to as Covalent Organic Frameworks (COFs).

One advantage of MOPs over MOFs is that they have much lower densities due to the fact they are comprised of solely lighter atoms (C, Si, N, O, B, H). It has been suggested in the literature that this decreased density will ultimately lead to products of relatively lighter mass for certain applications.⁶⁻⁸ Recent studies by Yaghi and coworkers produced boronate and boroxine Covalent Organic Frameworks (COFs) of high surface areas and H_{2(g)} uptake capacities. For example, self condensation of benzenediboronic acid (BDBA) forms a 2-D boroxine network, as does the condensation between BDBA and hexahydroxytriphenylene (Scheme 1-2). At the time these networks were in fact the highest recorded surface area of 1590 m²g⁻¹ for COFs and lowest reported densities for microporous materials of 0.58 g cm⁻³.^{6,7} More recently, 3-D COFs have been prepared

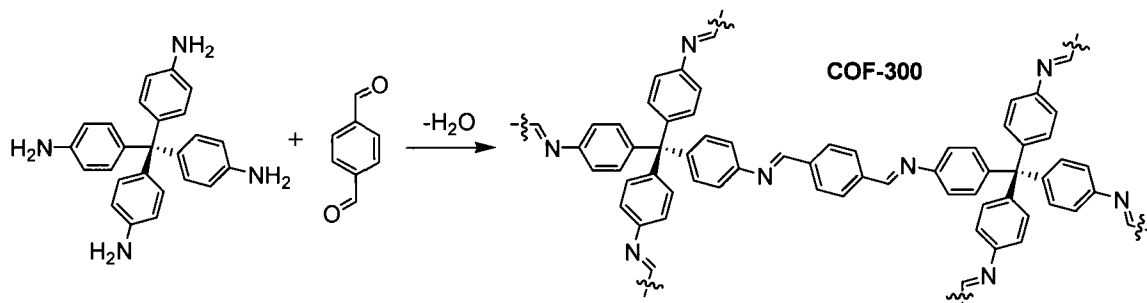
using appropriate boronic acid building blocks. These materials exhibit exceptionally high surface areas and low densities.³⁶

Scheme 1-2: Boronate ester and boroxine linked COFs



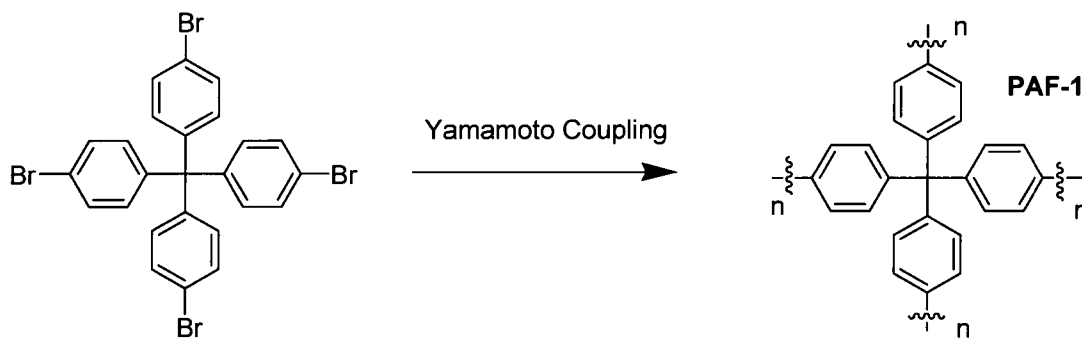
Yaghi has also produced impressive results by creating another COF linked together by imine bonds which showed a surface area of $1360 \text{ m}^2\text{g}^{-1}$ and pores with diameter of 7.8 \AA and a low density of 0.66 g cm^{-3} (Scheme 1-3).⁸

Scheme 1-3: Imine linked MOP.



Zhu *et al.* also published a report of a MOP with exceptionally high surface area and gas uptake capacity. These networks formed from tetra(phenyl)methane units employed the use of Yamamoto coupling (Scheme 1-4) and resulted in a BET surface area of $5600 \text{ m}^2\text{g}^{-1}$ and absolute $\text{H}_{2(\text{g})}$ uptake of 10.7% by weight at 77 K and 48 bar which is the highest reported surface area for a microporous material to date.¹⁰

Scheme 1-4: Yamamoto coupling formation of a Porous Aromatic Framework (PAF).



In order for a network to maintain permanent microporosity, it is thought that linking rigid building blocks at well-defined positions is an important factor. Consequently, aromatic molecular building blocks are often employed. There have been examples of imine linkers⁸ and boroxine and boronate esters^{6,7} which are also rigid imposing a planar geometry.

There are numerous advantages, and likewise disadvantages, associated with microporous organic polymers. The very high surface areas exhibited by MOPs could lead to useful applications, much like other materials exhibiting higher than usual surface areas have proven to, such as zeolites^{37,38} and MOFs.³⁹⁻⁴¹ Both have proven useful for catalysis, waste remediation and separation chemistry and it is logical to assume with similar or greater surface areas, thermal stability, and chemical diversity, that MOPs can be tailored to similar applications. In fact, there are waste water extraction examples of triptycene based frameworks selectively removing benzene from water.⁴² Additionally, due to the extremely high surface areas and gas uptake capacities,⁴³ MOPs are among the leading candidates for a practical hydrogen gas storage material.

Perhaps one of the most attractive features associated with MOPs is the synthetic diversity that is available. There are many examples of different chemistry used to create MOPs including Friedel-Crafts alkylation,⁴⁴ dibenzo-dioxane formation,⁴⁵ imidization,⁴⁶ amidation,⁴⁶ Sonagashira cross-coupling,⁹ homocoupling,⁴⁷ boroxine and boronate-ester formation,^{6,7} nitrile cyclotrimerization,⁴⁸ and Yamamoto coupling.¹⁰

In addition to the vast scope of synthetic possibilities, there are also extensive opportunities for post synthetic modifications due to the chemical and thermal stability and diversity of most MOPs.

1.5 Post Synthetic Modifications of Microporous Materials

Many porous materials including MOFs, PIMs, MOPs, activated carbons and zeolites have found applications in various fields such as catalysis, separations and gas storage causing interest to grow surrounding this class of solid-state materials.³⁹⁻⁴¹ In order to extend the uses of these materials it is important to increase the complexity and sophistication of the functionalities within the networks. By having the ability to modify the physical or chemical environment within the pores of microporous networks we are given the advantage of being able to tune a network's interactions with guest molecules making them increasingly tailored for specific applications.

While it is possible to place desired functionalities within a network by having the functionalities present on the building blocks before network formation, this approach can also present many problems. Often the formation of frameworks, especially crystalline ones, have very specific reaction conditions which cannot be altered and still produce quality networks.⁶⁻⁸ Therefore, it is often the case that a highly desired functionality is not compatible with network formation because it interferes, or is interfered with, for chemical, steric or thermal reasons.⁴⁹ Secondly, it can often be very time consuming and difficult to introduce a desired functionality to the building blocks, while it would simply be easier to form a network and add the functionality to the network after synthesis (Figure 1-3). Thus to avoid these limitations, it is very important to be able to tailor a framework post synthetically assuming that the network is sufficiently robust once created in order to introduce desired functionality.⁴⁹

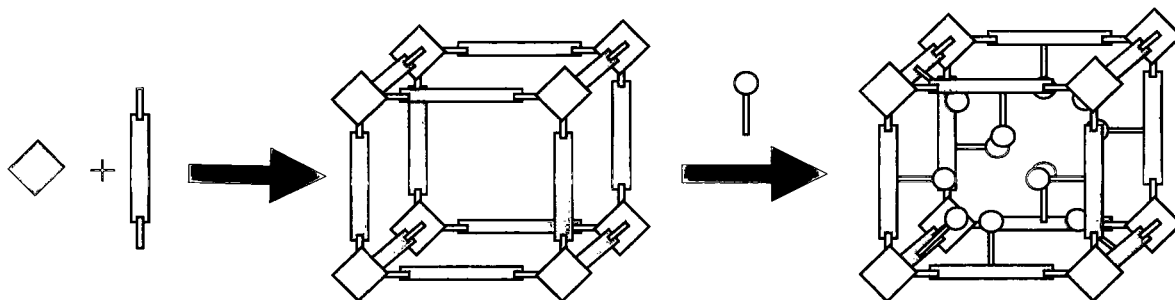


Figure 1-3: A general scheme illustrating the concept of post synthetic modifications to a porous framework.

There have been extensive examples of post synthetic modifications to MOFs via the covalent bonds of the organic struts between metallic nodes. The types of covalent post synthetic transformations to MOFs reported including amide coupling,⁵⁰⁻⁵² imine condensation,^{53,54} urea formation,⁵⁵ alkylation,⁵⁶ bromination,⁵⁷ reduction⁵⁸ and protonation.⁵⁹ For example, Cohen and co-workers have shown the acetylation of IRMOF-3 by targeting the amino groups present with acetic anhydride and larger acid anhydrides (Figure 1-4).

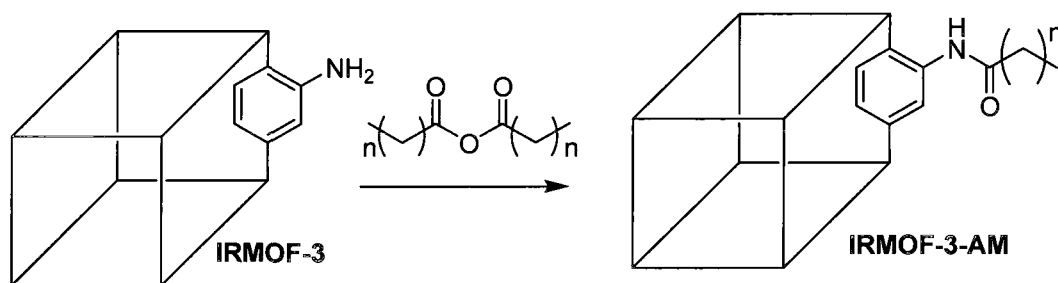


Figure 1-4: Scheme of representative post synthetic modification to IRMOF-3 with various anhydrides.

By attaching different length acetyl chains within the framework they were able to show that pore size can be tuned post synthetically.⁶⁰ Cohen then attempted acetylation with chiral acid anhydrides and successfully converted an achiral MOF into a chiral MOF.⁴⁹

Post synthetic modifications have also been employed with other solid state materials such as carbon nanotubes, zeolites, porous silicates, and the field of metal organic frameworks have been extensively explored.⁴⁹ For example, carbon nanotube post synthetic modifications have been studied in great detail⁶¹⁻⁶⁴ in order to increase their solubility in organic and aqueous solvents. These post synthetic modifications have allowed carbon nanotubes' dispersibility in solution to increase and make them more compatible with other materials for applications in molecular devices.⁶⁵ There have also been extensive investigations involving the functionalization of mesoporous silicas. Reactive (-SiOH) groups lining the pores allow for the grafting of organic functional groups in order to tailor the frameworks.⁶⁶ To date there have been no reports of post synthetic modifications to purely organic based frameworks such as MOPs or COFs.

1.6 Research Objectives

The overall objective of this research is to prepare new microporous materials from organic building blocks and to control the properties of these materials. The specific objectives of the research are:

- 1) The preparation of boronate ester networks using triptycene building blocks. Triptycenes are rigid and should impart robustness during network formation, while

boronate esters have been shown to form favourable crystalline networks in a well ordered manner. These are described in chapter 2.

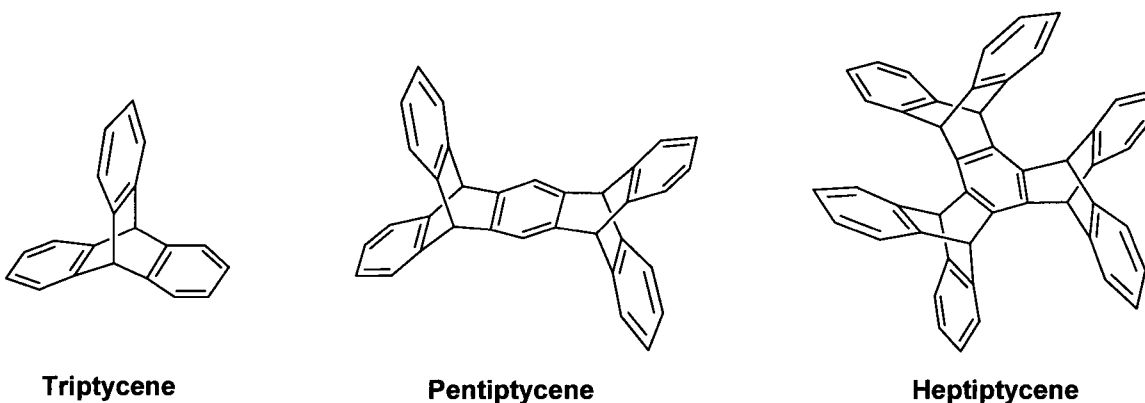
2) The preparation of an imine linked network and post synthetic modification of this imine functionality. The modifications were performed first via reduction of the imine bonds within the network to increase chemical stability followed by subsequent acetylation in order to control the pore volume within the network. Presented in chapter 3, this study represents the first post synthetic modification of a purely organic microporous material.

3) The preparation of new PAFs based on a tetraphenylbimesityl core and then the exploration of post synthetic modifications to PAFs through electrophilic aromatic substitution. These results are described in chapter 4.

Chapter 2: Novel Triptycene Based Framework

2.1 Introduction

Iptycenes, first synthesized in 1942,⁶⁷ consist of phenyl rings joined together by a [2.2.2]bicyclooctatriene bridgehead system. According to the nomenclature adapted by Hart, iptycenes are named based on the number of arene rings present, separated by the bridgeheads. Thus, triptycene consists of three phenyl rings joined together by a [2.2.2]bicyclooctatriene bridgehead.⁶⁸



Triptycene was chosen as the building block of a novel microporous polymer because iptycenes exhibit three properties making them especially useful for supramolecular chemistry: their rigidity, multibladed geometry and presence of aromatic rings. Due to the high energy barrier to twisting and deformations of iptycenes, they provide the required rigidity that is necessary for a supramolecular network to maintain pores and remain intact upon the removal of guest molecules. Secondly, the multibladed geometry of iptycenes hinders efficient packing between molecules and makes them especially useful for creating “free volume” within a network. Finally, the aromatic rings present in iptycenes are capable of engaging in interactions with guest molecules through

means of intermolecular interactions with the π -system, making them useful for storage or separation applications.^{67,69} For example, Yang and Swager prepared poly(phenylene-ethylene)s (PPEs) with pentyptycene backbones that prevented π stacking between monolayers and greatly increased the solubility of polymers in organic solvents and fluorescence quantum yield. This led to the creation of thin films of these polymers which demonstrated rapid, reversible and highly sensitive detection of nitro-aromatic explosives such as TNT via fluorescence quenching. This is a result of the pentyptycene creating a highly porous polymer with cavities able to be penetrated by analyte vapours which then interact with the electron rich backbones.⁷⁰

There have been several polymers of intrinsic microporosity (PIMs) reported in which an iptycene monomer was employed in the design and synthesis.⁷¹⁻⁷⁵ A notable example being the previously mentioned work by McKeown (Scheme 1-1).³⁰

Since the introduction of covalent organic frameworks to the field of microporous materials by Yaghi, it has been of growing interest to synthesize new covalent organic frameworks with high surface areas and guest uptake capacities.⁶⁻⁸ However, there are several issues to consider when constructing such a network. One would like the building blocks to be rigid enough to not collapse after synthesis and also remain intact after guest exchange or evacuation of pores within the network. For certain applications it is also of importance to form well-ordered networks so that pores are of uniform sizes. This could potentially lead to applications in gas storage⁷⁶ or waste removal.⁷⁰

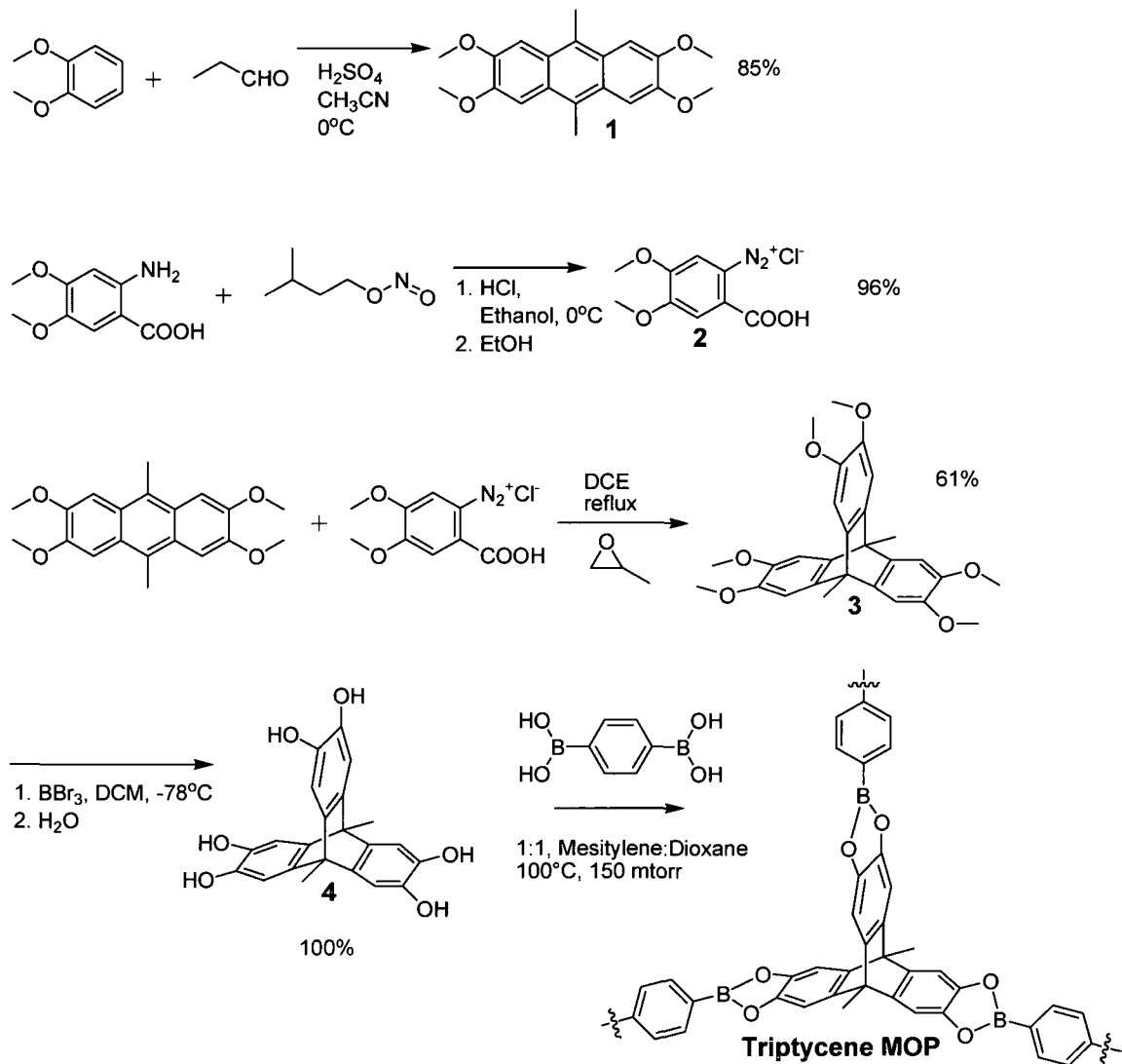
Since the condensation reaction between boronic acids and diols to form boronate esters is reversible, it is anticipated that networks formed using these reactions will avoid awkward network topologies in favour of well-ordered networks. The use of triptycene

and benzene based building blocks should provide sufficient rigidity while the triangular shape of triptycene should allow for free space to form within the network. Thus, it is hoped the use of triptycene monomers in combination with boronic acid alcohol condensation will result in a novel covalent organic framework of high surface area and guest molecule uptake.

Within this chapter, I will describe the attempted synthesis of a framework based on hexahydroxytriptycene and benzenediboronic acid (BDDBA) building blocks via the condensation of alcohol functional groups.

2.2 Synthesis

Scheme 2-1: Synthesis of Triptycene MOP



The synthesis began, as shown in Scheme 2-1, with a reaction between veratrole and acetaldehyde, in the presence of acetonitrile and concentrated sulphuric acid, to form 2,3,6,7-tetramethoxy-9,10-dimethylantracene (**1**) in 85% yield.⁷⁷ A benzyne precursor was also synthesized using 2-amino-4,5-dimethoxybenzoic acid, which was treated with

isoamyl nitrite in the presence of concentrated HCl in order to produce a diazonium salt **(2)**, in 96% yield.⁷⁸ These two products were then used together in a Diels-Alder reaction in order to yield **(3)** in 61%.⁷⁸ The methoxy groups of **3** were subsequently cleaved using BBr₃ resulting in hydroxyl functionalized triptycene building block **(4)** in near quantitative yield.⁷⁸

Compound **4** was then reacted with BDBA following a procedure adapted from Yaghi's method for COF synthesis.^{6,7} Both reactants were suspended in a 1:1 mixture of mesitylene and dioxane within a sealed pyrex tube and evacuated to 150 mtorr of pressure before being sealed and subsequently heated at 100°C for 3 days. The resulting solid, which was insoluble in all solvents, was filtered and washed thoroughly with THF in order to ensure all starting materials had been removed.

The solid network obtained was characterized via infrared spectroscopy, powder X-ray diffraction, thermogravimetric analysis and nitrogen gas adsorption experiments.

In addition to synthesis of **Triptycene MOP**, a model compound was synthesized from a condensation between **4** and phenyl boronic acid as shown in Scheme 2-2.

The IR spectrum of model compound **(5)** (Figure 2-1) shows strong absorption bands at 1353 cm⁻¹ and 1024 cm⁻¹ which are characteristic of B-O stretching.^{6,7} This model compound was used as a point of comparison for IR absorptions in **Triptycene MOP**.

Scheme 2-2: Synthesis of triptycene model compound 5.

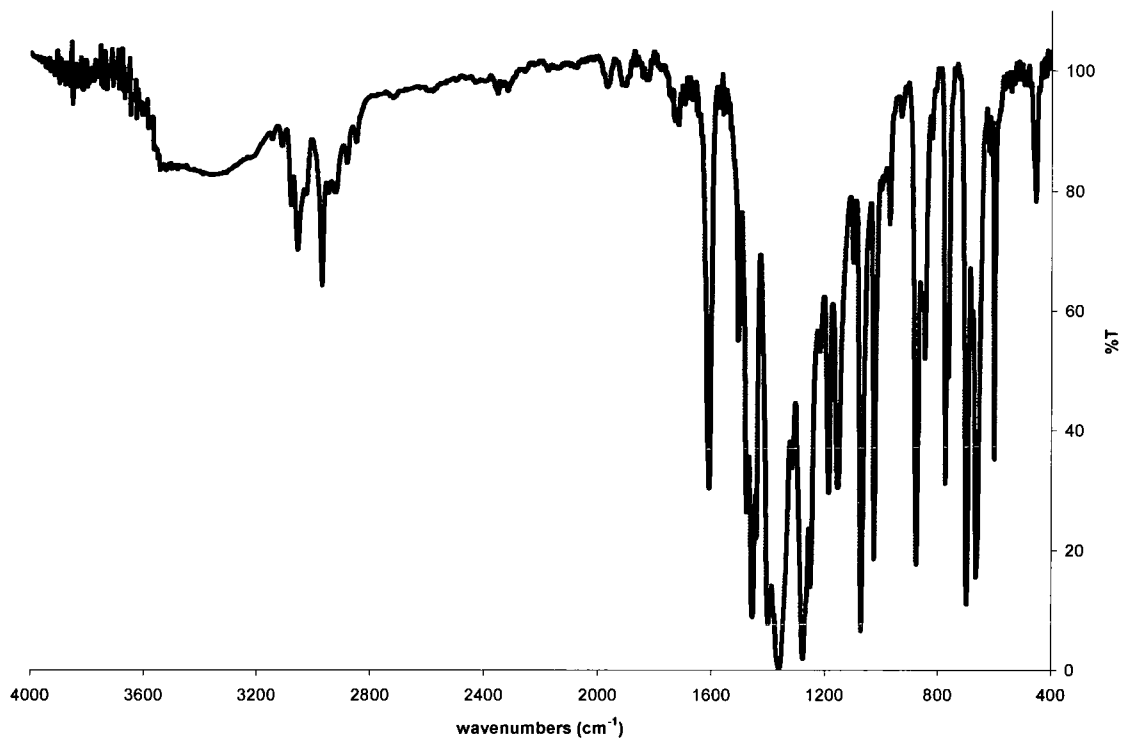
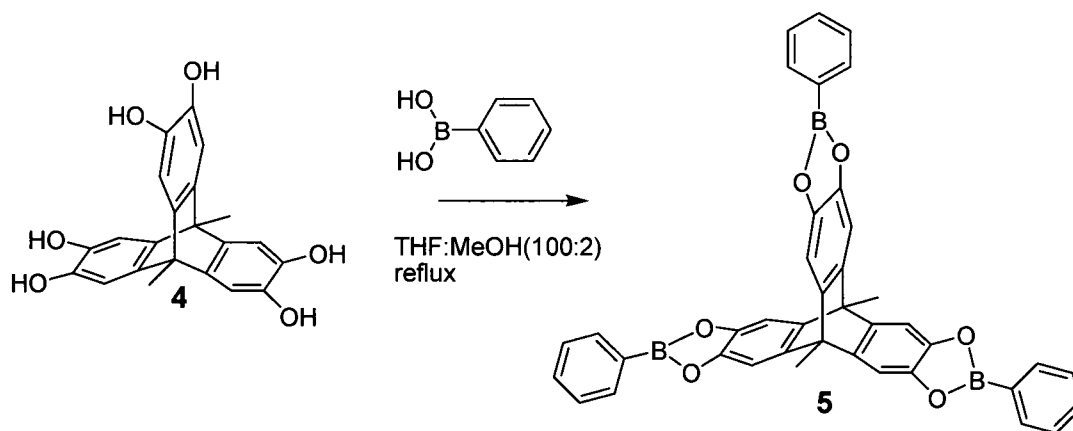


Figure 2-1: IR spectrum of model compound 5.

2.3 Results and Discussion

The infrared spectrum of **Triptycene MOP** (Figure 2-2) shows the appearance of several characteristic peaks in the boronate network, as well as the disappearance of several peaks that were observed in the starting materials. Namely, two peaks which appear in framework one at 1031 cm^{-1} and 1348 cm^{-1} are characteristic of boronate ester stretching and are not present in either of the starting materials. Additionally, there is the disappearance of the peak at 1698 cm^{-1} in the IR spectrum of the triptycene building block and the moderate abatement of the OH stretch at approximately 3300 cm^{-1} in the spectrum of **Triptycene MOP**. Both provide further evidence for the successful formation of **Triptycene MOP**. However, the significant OH stretching band in the product suggests that many hydroxyl sites remain unreacted.

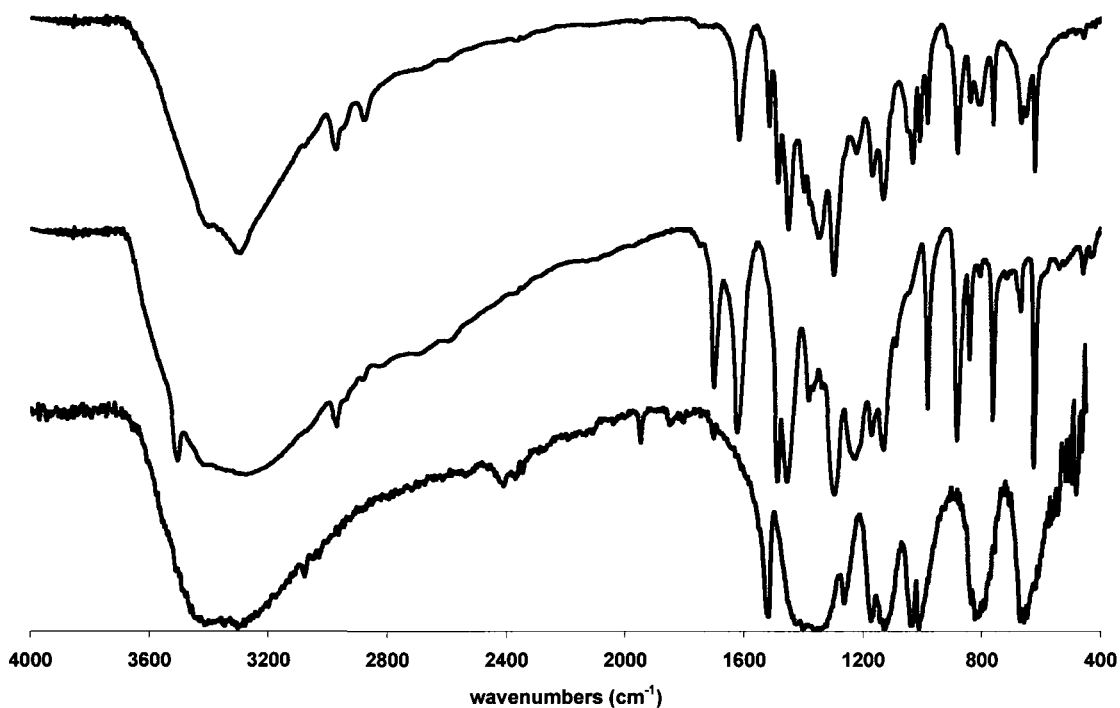


Figure 2-2: IR spectrum of **Triptycene MOP** (green line), and starting materials benzenediboronic acid (blue line), **4** (red line).

While it was hoped that the newly formed network would be microcrystalline, powder X-ray diffraction studies showed no crystallinity within the material. Thus, the network has formed in a random and poorly defined manner, resulting in an amorphous rather than crystalline material.

Nitrogen gas adsorption experiments performed on **Triptycene MOP** showed a sharp uptake of approximately $60 \text{ cm}^3\text{g}^{-1}$ at very low relative pressures, indicative of a microporous material. Gas adsorption experiments provided a BET surface area of $200 \text{ m}^2\text{g}^{-1}$. As shown in Figure 2-3, some hysteresis between adsorption and desorption

isotherms is exhibited by the material suggesting that **Triptycene MOP** is flexible to a certain degree.

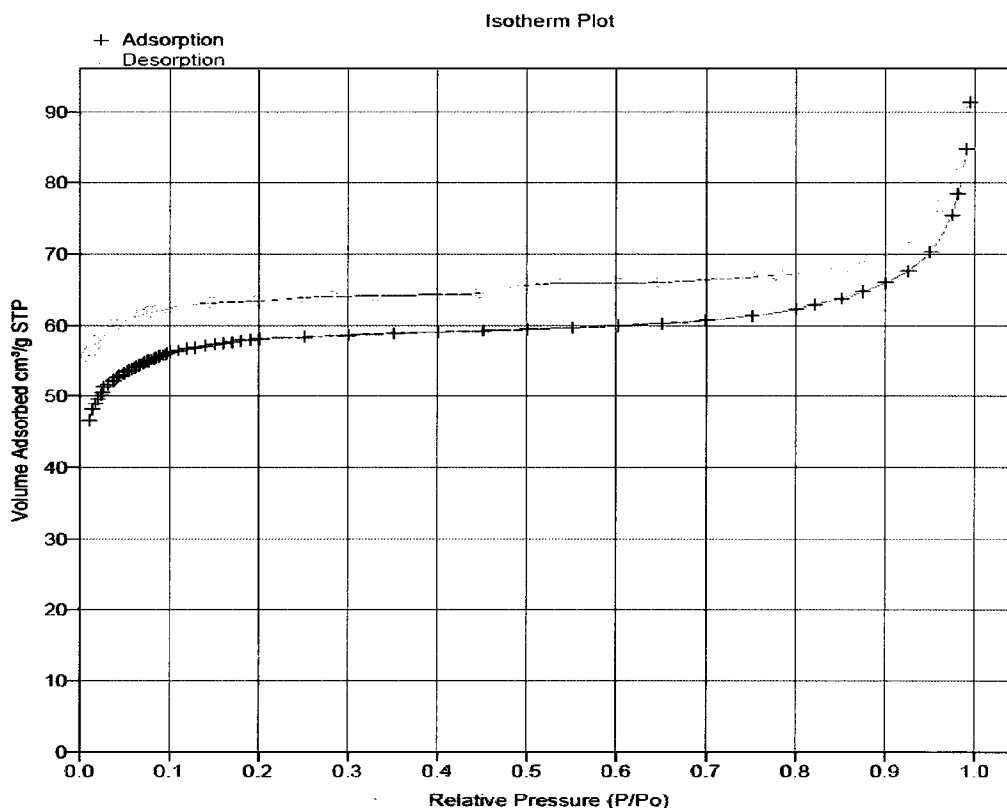


Figure 2-3: Nitrogen isotherm plot of **Triptycene MOP**. Adsorption points (black crosses), desorption points (red circles).

In addition to gas adsorption experiments, thermogravimetric analysis of **Triptycene MOP** was carried out using several different solvents in order to test the uptake capacity of the material. Figure 2-4 shows the thermogravimetric studies of **Triptycene MOP** after being synthesized, submerged in several solvents individually, and finally being activated. The solvent uptake experiments show a mass loss of up to 17% below 200 °C suggesting the pores within **Triptycene MOP** are capable of swelling to uptake a significant amount of guest molecules and provides complimentary support to

the network being permeable to reactants. As expected, after being activated the plot shows minimal mass loss suggesting all solvent has been evacuated from the pores within **Triptycene MOP**. Finally, thermogravimetric analysis experiments show that the network is thermally stable at temperatures up to 400 °C.

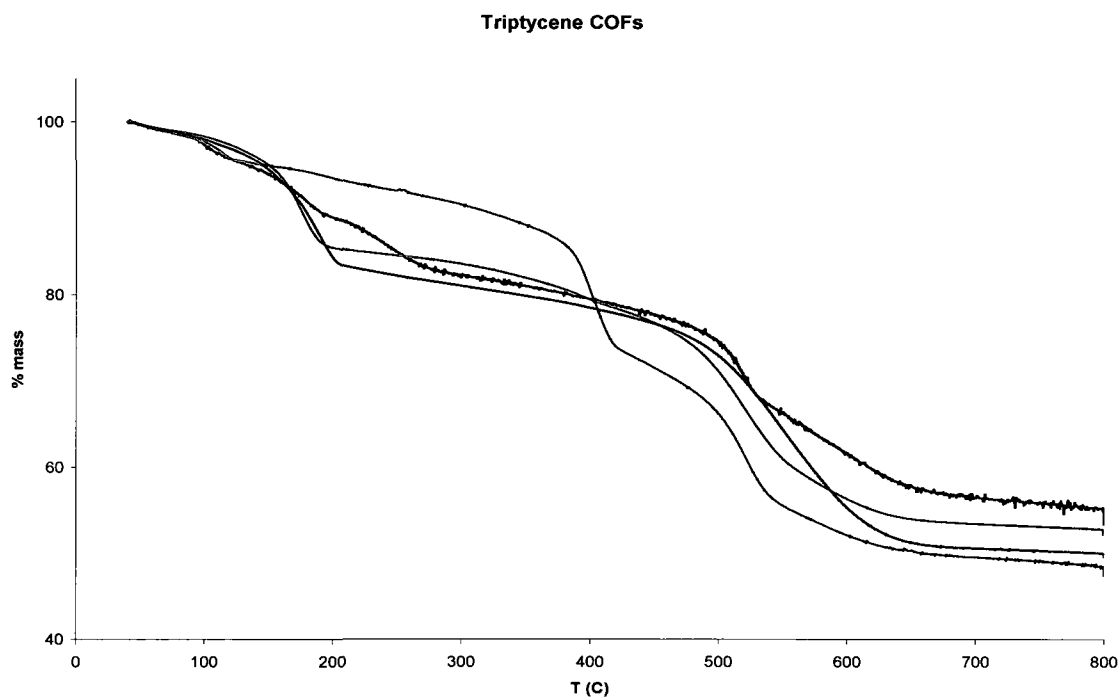


Figure 2-4: Thermogravimetric analysis of **Triptycene MOP**. Triptycene MOP as synthesized (dark blue), activated (light blue), ether guest exchange (pink), toluene guest exchange (green).

An interesting observation is that there appears to be a steady mass loss in the activated **Triptycene MOP** between 100 °C and 400 °C. This could potentially be attributed alcohol and boronic acid functional groups, still present on the ends of the amorphous network, which may undergo further condensation under the high temperature conditions to evolve $\text{H}_2\text{O}_{(g)}$. It could also correspond to decomposition of the network.

It should also be noted that in an attempt to perform guest exchange within the pores using acetone, **Triptycene MOP** slowly degraded presumably due to hydrolysis of the B-O bonds. This observation was studied in greater detail through guest exchange of Yaghi's COF-1 (Scheme 1-2) with acetone. Similar to **Triptycene MOP**, the B-O bonds of COF-1 were hydrolysed and the network subsequently broke apart. These observations suggest that COFs based on boroxines and boronate esters have limited stability which could ultimately limit their use in applications, such as hydrogen fuel storage tanks. Similar observations have been reported in the literature that support our conclusions.⁷⁹

2.4 Summary

In summary, a novel organic framework based on the condensation between benzenediboronic acid and diol substituted triptycene has been created. While the network was not crystalline, it did exhibit permanent microporosity. The material was shown, via thermogravimetric and gas adsorption analysis, to have a guest uptake capacity of 17% by mass as well as a BET surface area of $200 \text{ m}^2\text{g}^{-1}$. Despite this novel framework failing to exhibit high surface areas it is nonetheless an important study resulting in a new material. Due to the moisture sensitivity of the boroxine bonds within the network it is most likely that networks formed in this manner would not find use in applications.⁷⁹ Thus it is important to study networks that are not sensitive to hydrolysis, such as those formed by metal catalyzed cross couplings, in order to create frameworks useful for applications such as gas storage, catalysis or separations.

Chapter 3: Post Synthetic Modifications to an Imine Linked MOP

3.1 Introduction

The ability to tailor the properties of microporous materials, specifically incorporating desired functional groups within the networks, can be a challenging aspect of their synthesis. In order to incorporate a functional group into a network it is often required that the functionality be attached to the molecular building blocks prior to network formation.⁴⁹ In order for this to be possible, the functional groups must also be compatible with the reaction conditions employed. This is often difficult because the reaction conditions required for the formation of microporous networks such as temperatures, pressures, reactants or solvents used are often incompatible with the desired functionality. It is also possible that simple steric reasons prevent the network from forming in its most desired state when larger functional groups are involved. For these reasons, covalent post synthetic modification is an attractive alternative approach for incorporating functional groups into microporous materials.

Within this chapter I will describe the synthesis and characterization of an imine linked MOP, and the first post synthetic modification of a purely organic microporous network linked together by imine bonds.

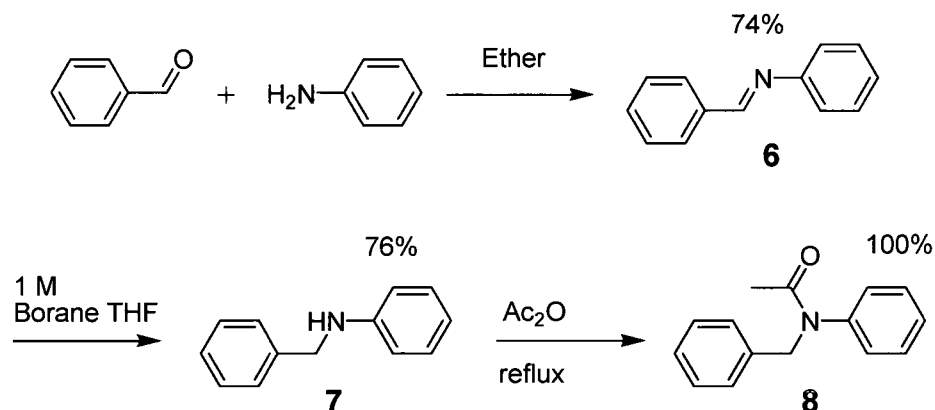
The imine linked MOP provides us with a distinct functionality to which we can perform post synthetic modifications via reduction of the imines to amines. Additionally, further post synthetic modifications are possible by acylating the amines into amide groups. The goal is to show that we can provide access to new microporous materials with diverse characteristics and controllable properties. Specifically, we hope to show that it is possible to reduce the imine linkers to amine bonds which should be more

resistant to hydrolysis. We then hope to acetylate the amine bonds, in effect tuning the pore size within the network while also showing that sequential post synthetic modifications are possible.

3.2 Model Studies

In order to first test the feasibility of the post synthetic modifications to be performed on the microporous covalent network, model compounds were synthesized and characterized.

Scheme 3-1: Model reactions.



Benzaldehyde and aniline were stirred in ether for several hours in order to form the imine linked *N*-benzylidenebenzenamine (**6**) in 74% yield (Scheme 3-1). Compound **6** was treated with 1M borane-THF complex in order to reduce the imine bond to form *N*-benzylbenzenamine (**7**) in 76% yield. Finally, **7** was heated at 100 °C in Ac_2O for one hour to yield *N*-benzyl-*N*-phenylacetamide (**8**) in a quantitative yield. These compounds were characterized by ^1H NMR and IR spectroscopy which is consistent with literature data.^{80,81} Particularly important for characterization of the corresponding networks are the

IR spectra, which provide a basis for comparison. Notable IR peaks of **6** appear at 1625 cm^{-1} and 1191 cm^{-1} , both of which correspond to a C=N imine bond. It is evident that upon reduction these peaks are no longer present in **7**, while a new strong broad peak appears at 3415 cm^{-1} corresponding to N-H stretching again proving evidence of the reduction. Finally, after acetylation of the model compound, the IR spectrum of **8** shows a new strong, broad peak at 1650 cm^{-1} consistent with an amide carbonyl and an almost complete disappearance of the N-H stretch peak present in **7** (Figure 3-1).

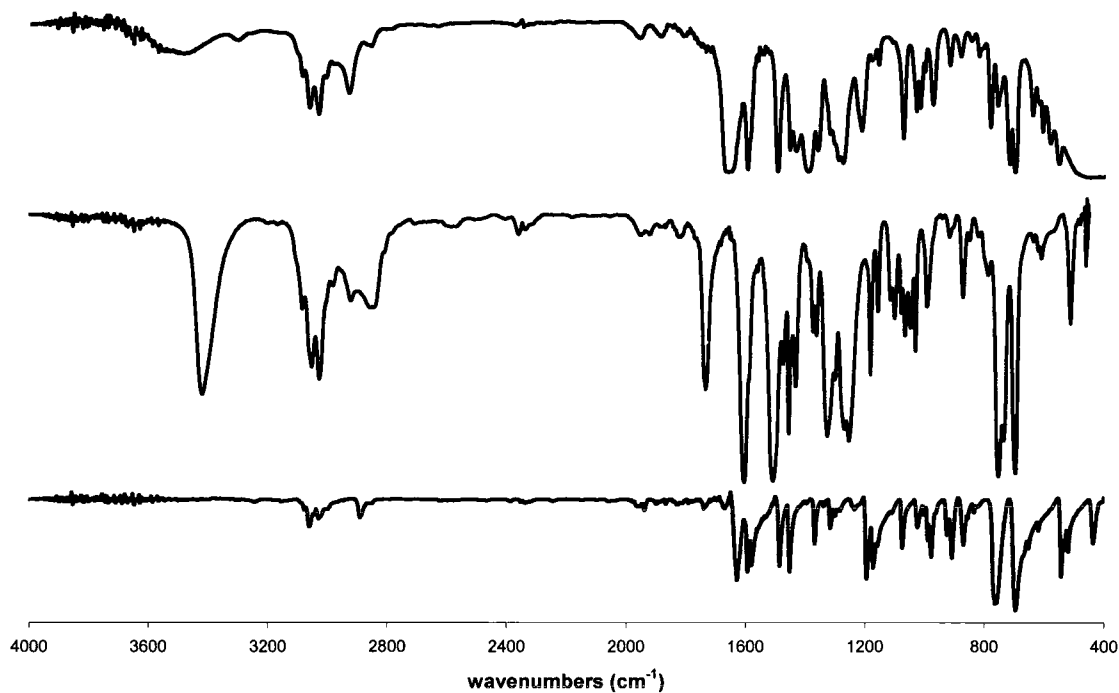
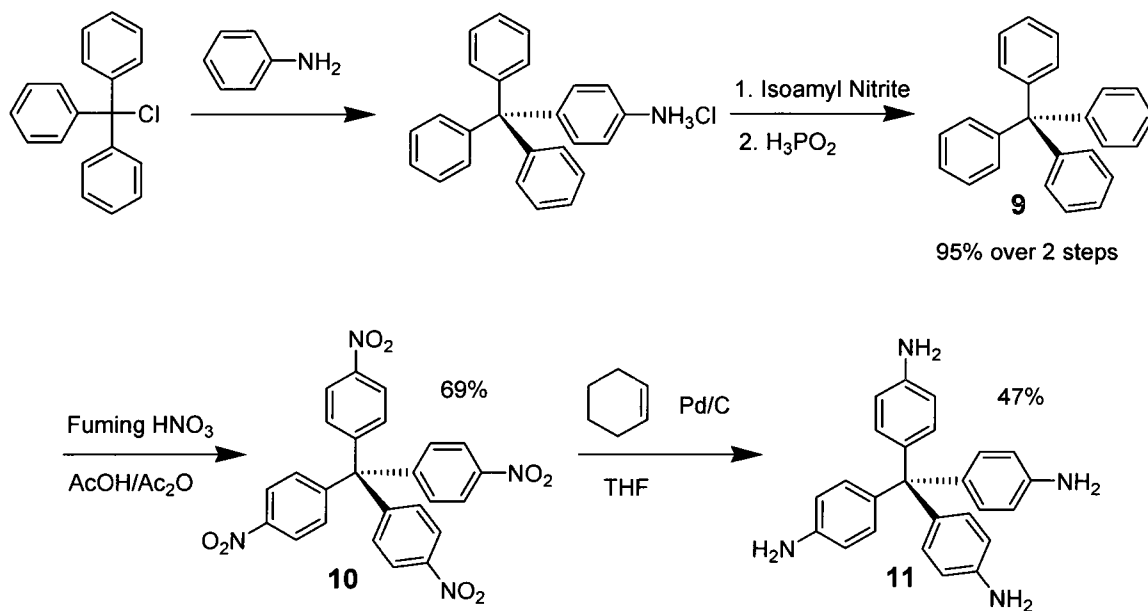


Figure 3-1: Infrared spectrum of model compounds **6** (blue line), **7** (red line), **8** (black line).

3.3 Synthesis

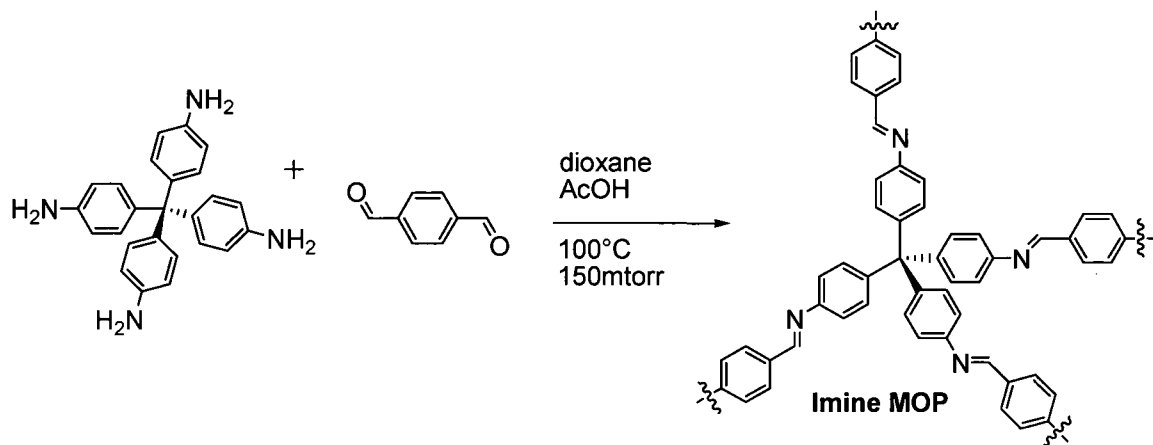
The tetrakis(4-aminophenyl)methane (**11**) building block was synthesized based on previously reported literature procedures,⁸² outlined in Scheme 3-2, beginning with a neat reaction between trityl chloride and aniline. Upon treatment with isoamyl nitrite, followed by hypophosphorous acid, tetraphenylmethane (**9**) is yielded in 95% over two steps. The phenyl rings were then nitrated in the para position using fuming nitric acid in a mixture of AcOH and Ac₂O to yield **10** in 69%, which was subsequently reduced using cyclohexene as a source of hydrogen over Pd/C as a catalyst in 47% yield. This yielded the desired tetrakis(4-aminophenyl)methane **11** building block in 31% overall yield.

Scheme 3-2: Synthesis of tetrakis(4-aminophenyl)methane building block **11**.

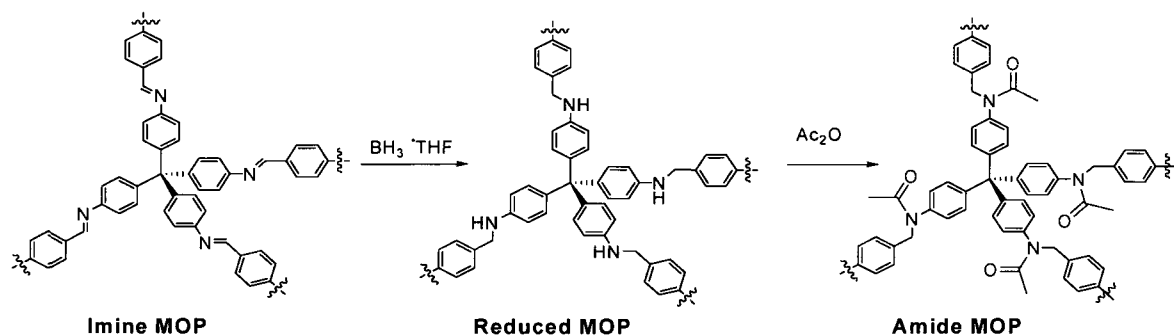


The synthesis of the **Imine MOP**, based on work previously reported by Yaghi,⁸ was carried out by reacting terephthalaldehyde with tetrakis(4-aminophenyl)methane in order to form an extended 3D porous framework (Scheme 3-3).

Scheme 3-3: Synthesis of **Imine MOP**.



Scheme 3-4: Reduction and acetylation of **Imine MOP**.



3.4 Characterization of Networks

The formation of **Imine MOP** was confirmed by IR spectroscopy and ^{13}C CP-MAS solid state NMR spectroscopy (Figures 3-2 and 3-3). The results are consistent with previously reported data.⁸ There are matching signals in the IR spectrum of model compound **6**, **Imine MOP** and that of Yaghi's COF-300 from at 1625 cm^{-1} identifying the imine bonds present. It is also important to mention that the strong broad band at 3450 cm^{-1} present in the IR spectrum of **Imine MOP** is also present in Yaghi's COF-300. While this signal suggests that there are still NH_2 groups present it is not unexpected as this identifies the ends of the frameworks. The ^{13}C CP-MAS solid state NMR spectrum of **Imine MOP** matches Yaghi's results in all aromatic signals as well as the other two major diagnostic signals at 159 ppm and 67 ppm corresponding to the imine carbons and central methane carbons present in the network.

Further investigation by powder X-Ray diffraction showed that, in contrast to Yaghi's crystalline and multiply interpenetrated COF, **Imine MOP** diffracted very weakly, with broad reflections suggesting mostly amorphous material.

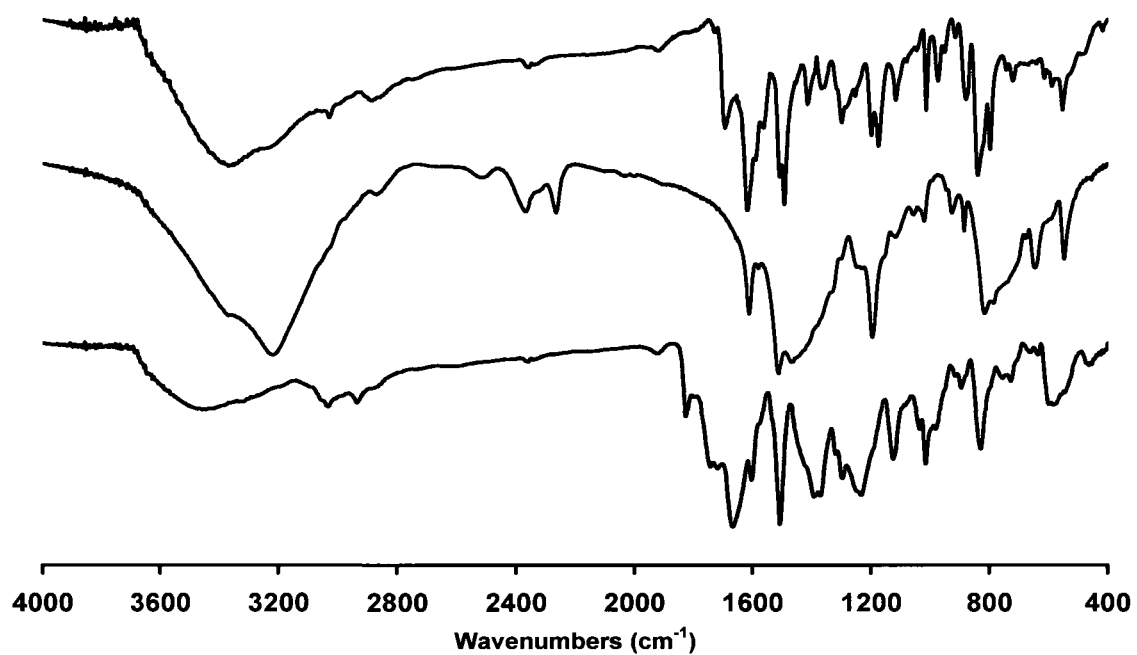


Figure 3-2. Infrared spectra of **Imine MOP** (black line), **Reduced MOP** (red line), and **Amide MOP** (blue line).

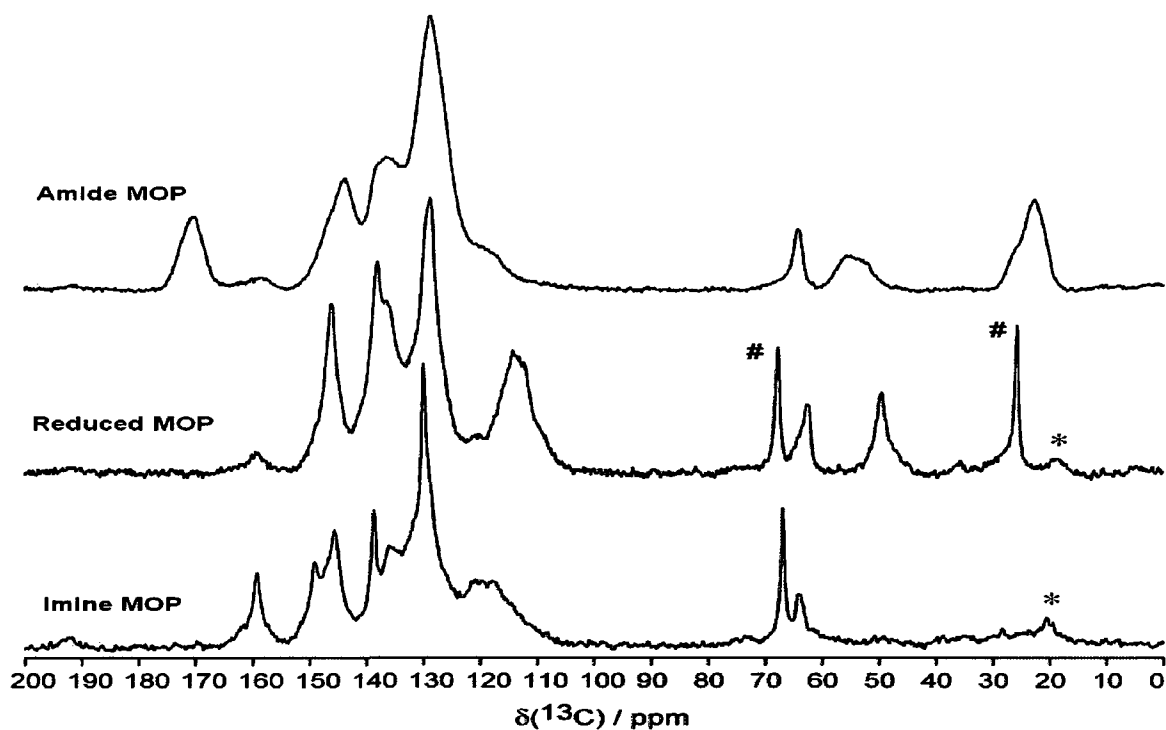


Figure 3-3. ^{13}C CP-MAS spectra of **Imine MOP**, **Reduce MOP**, and **Amide MOP**. Signals marked with * indicate spinning side bands, while the two signals marked with # for the spectrum of **Reduced MOP** correspond to included THF.

Upon being solvated with THF, thermogravimetric analysis of **Imine MOP** showed a mass loss of approximately 10% below 100 °C corresponding to the loss of solvent (Figure 3-4). Subsequent activation under heating at 100 °C under vacuum overnight, followed by resolution in THF showed similar results as compared to the original solvated framework, suggesting that the material has void spaces that can accommodate guest molecules.

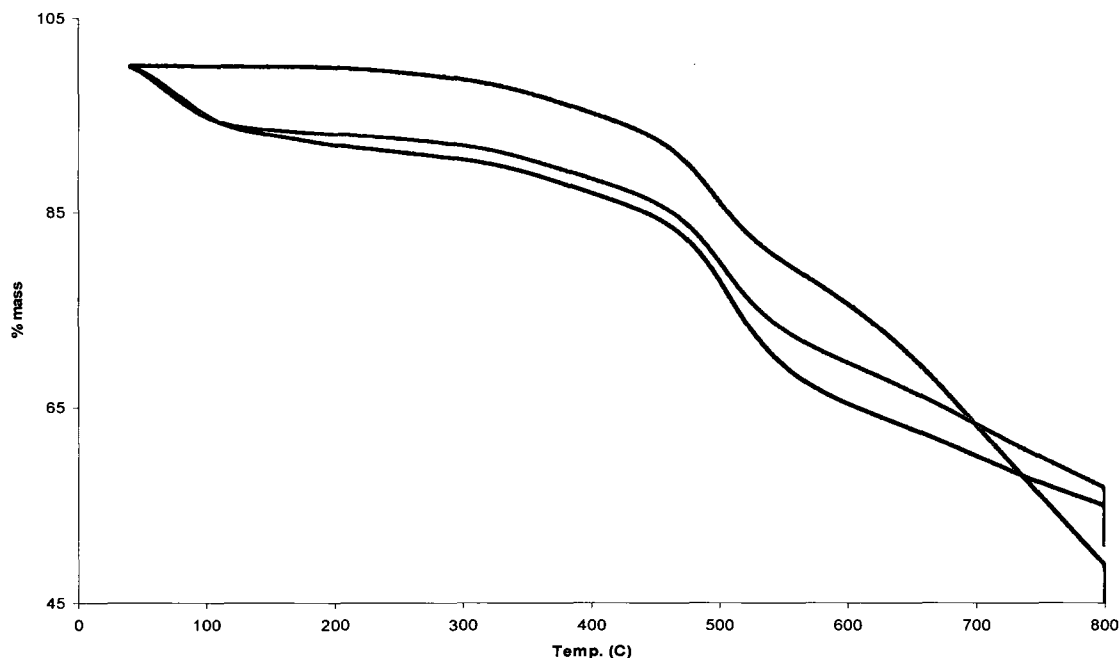


Figure 3-4. TGA traces of **Imine MOP** with THF (blue line), activated (black line), and resolvated with THF (green line).

Evidence for the permanent microporosity of **Imine MOP** was provided by nitrogen adsorption experiments (Figure 3-6). These experiments showed sharp uptake of nitrogen at low pressures which is indicative of a material with permanent microporosity. From the adsorption data the BET surface area was calculated to be $416 \text{ m}^2\text{g}^{-1}$. Although this value is substantially lower than COF-300 created by Yaghi, which showed a BET surface area of $1360 \text{ m}^2\text{g}^{-1}$, it does still demonstrate permanent microporosity of the material. There is some observed hysteresis between the adsorption and desorption isotherm which is again consistent with the work of Yaghi and coworkers and can be explained by some flexibility in the network.

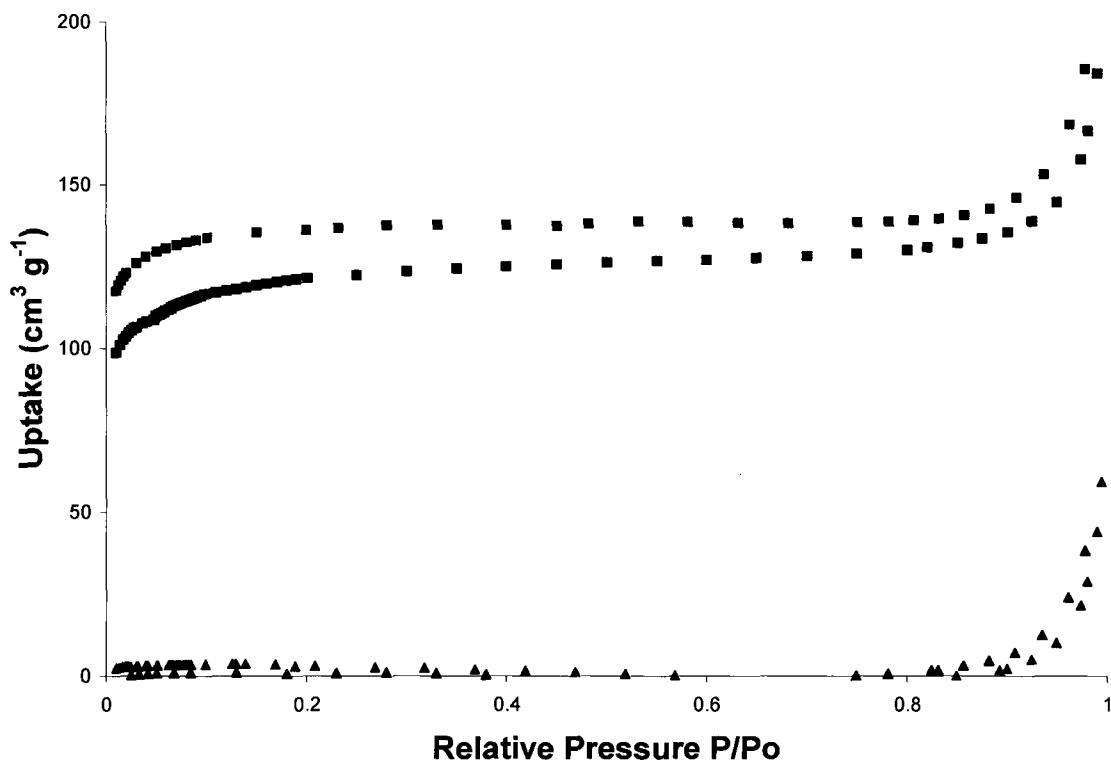


Figure 3-5. Nitrogen adsorption isotherm for **Imine MOP** (dark blue squares – adsorption, light blue squares – desorption) and **Reduced MOP** (light green triangles – adsorption, dark green triangles – desorption) measured at 77 K.

Reduced MOP was synthesized by suspending **Imine MOP** in 1 M borane-THF complex and stirring for 24 hours. After 24 hours of stirring the solution was quenched with water and the solid was filtered, washed thoroughly with water and THF, collected and dried under vacuum at 100 °C in order to remove all solvent. An infrared spectrum of the material (Figure 3-2) showed substantial attenuation of the C=N stretching band at 1615 cm^{-1} and a concomitant increase in the N-H stretching band at approximately 3200 cm^{-1} . These results are consistent with reduction of the imine bonds within **Imine MOP** resulting in the corresponding amines.

Further evidence of the reduction was confirmed by ^{13}C CP-MAS NMR spectroscopy (Figure 3-3), which displayed a virtual complete disappearance of the imine carbon signal at 159 ppm and the appearance of a new signal at 50 ppm corresponding to the benzylic carbon of the reduced product. These signals are consistent with the model compounds *N*-benzylideneaniline and *N*-benzylaniline which show respective imine and benzylic carbon peaks at similar chemical shifts. Both spectroscopic results show nearly complete reduction of the imine bonds within **Imine MOP**, indicating that the reducing agent has successfully penetrated the pores of the network and reacted with interior imine sites as well as the exterior sites.

Gas adsorption experiments of **Reduced MOP** (Figure 3-5) showed negligible uptake of nitrogen and gave a very small BET surface area of only $10\text{ m}^2\text{g}^{-1}$, suggesting that the permanent microporosity of the material had been lost upon the reduction of the network. This observation can be attributed to the increased flexibility of the bonds within the reduced network. **Imine MOP** which was previously held together by rigid carbon nitrogen double bonds has now been reduced to flexible carbon nitrogen single bonds which results in the collapse of the network onto itself upon evacuation of included solvent, and thus permanent microporosity is lost.

However, thermogravimetric analysis of **Reduced COF** (Figure 3-6) shows comparable thermal stability to **Imine MOP** with substantial decomposition at temperatures above $400\text{ }^\circ\text{C}$. Solvation, activation and resolvation of **Reduced MOP**, again shown by TGA, also demonstrated similar solvent uptake capacity to that of **Imine MOP**, with an uptake by mass of approximately 10%. So, while **Reduced MOP** did not demonstrate permanent microporosity, these observations by TGA results do suggest that

the material is still permeable and is able to swell in the presence of solvents retaining its ability to uptake guest molecules.

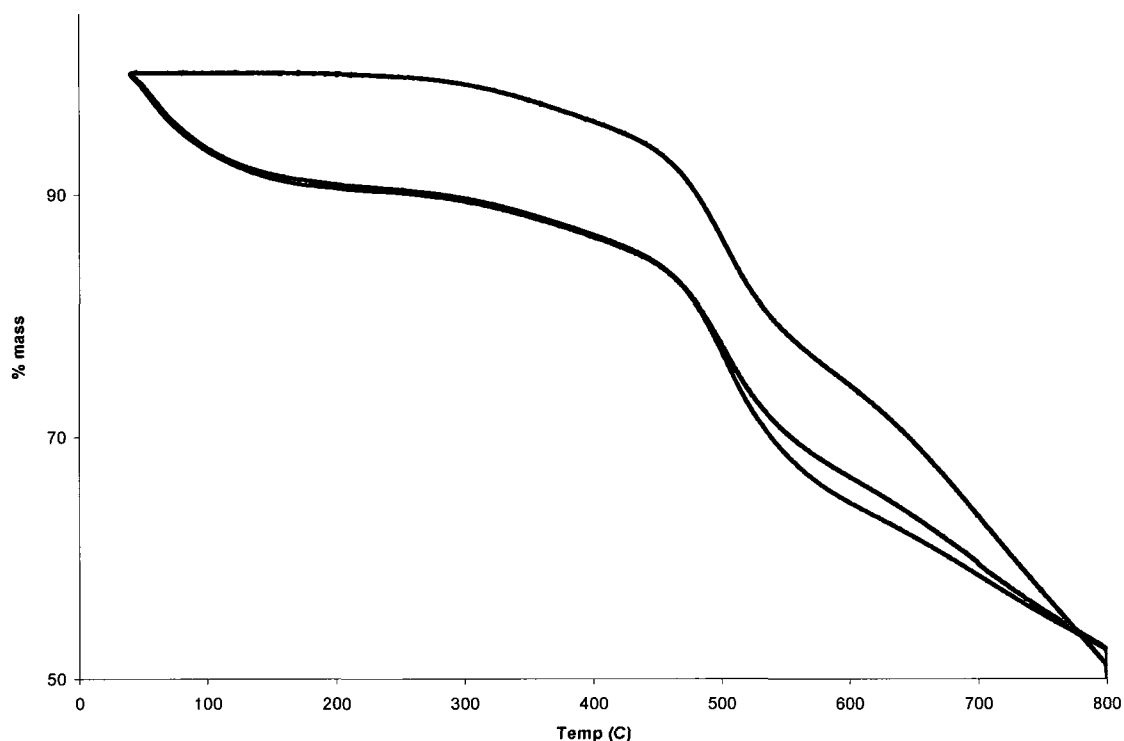


Figure 3-6. TGA traces of **Reduced MOP** with THF (blue line), activated (black line), and resolvated with THF (green line).

The stability of **Imine MOP** and **Reduced MOP** were also tested under aqueous acidic conditions in order to demonstrate the increased chemical stability towards hydrolysis of the reduced amine bonds. **Imine MOP** immediately decomposed after being heated at 40 °C in 2 M HCl. The network was presumably hydrolyzed to its corresponding starting materials, evident from the dissolution of the network. **Reduced MOP** on the other hand, remained intact and insoluble upon being heated at reflux for three hours. After recovering the material of **Reduced MOP** which was subjected to

these acidic conditions an infrared spectrum of the material showed a very broad N-H stretch from 3600 cm^{-1} to 2000 cm^{-1} characteristic of ammonium salts⁸³ (Figure 3-7). This result suggests that the amine bonds within the network were protonated, which is consistent with expectations. These observations suggest that similar materials could ultimately give rise to novel permeable ionic networks, with possible uses for ion separation or waste remediation.

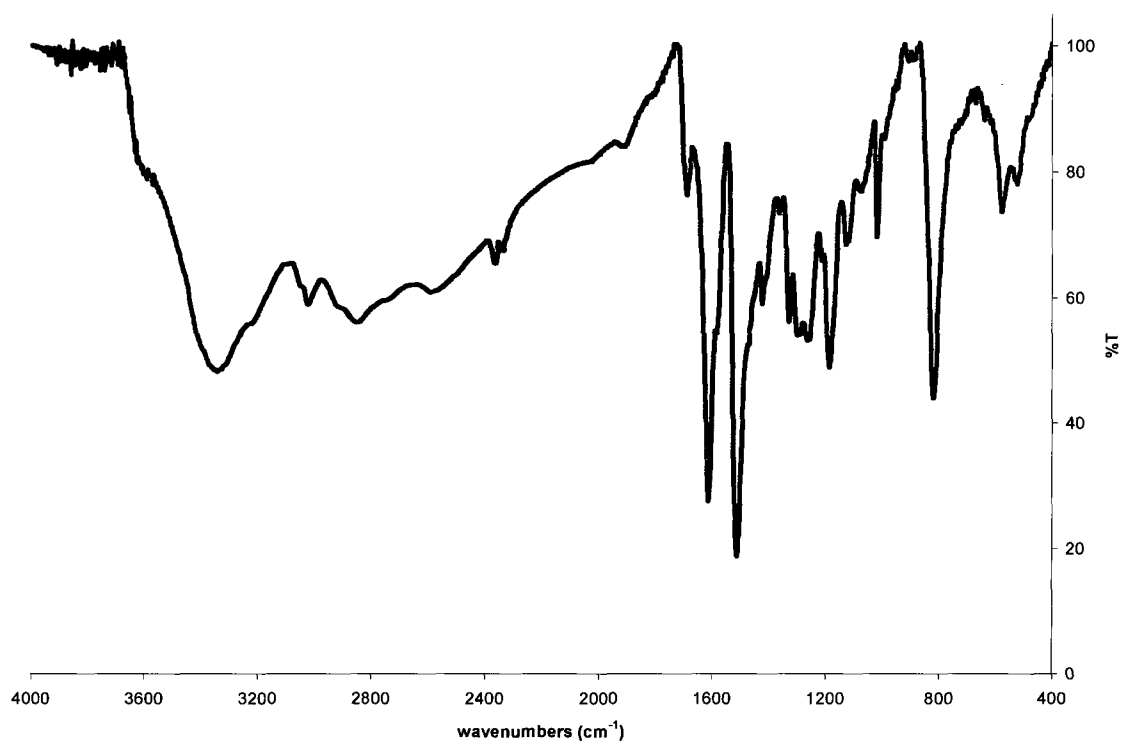


Figure 3-7. Infrared spectrum of **Reduced MOP** after being subjected to aqueous acidic conditions.

The amine bonds now present in **Reduced MOP** not only increase the chemical stability of the network but also provided functionality lending itself to possible further post synthetic modifications to the network. In order to show that further post synthetic

modifications were possible, the acylation of amine bonds using acetic anhydride was attempted. **Reduced MOP** was immersed in acetic anhydride for 24 hours at room temperature in order to allow the reactant to permeate into the pores of the network, followed by subsequent heating at 100 °C for 12 hours in a sealed pressure tube. After cooling to room temperature the solid was filtered and washed with copious amounts of water and THF, dried under vacuum and collected as **Amide MOP**. Again evidence of the post synthetic modifications were shown by IR and ¹³C CP-MAS NMR spectroscopy (Figures 3-2 and 3-3 respectively). In addition to the substantial decrease in the N-H stretching band, IR spectroscopy showed the appearance of a strong band at 1658 cm⁻¹, which is consistent with an amide carbonyl, C=O, stretch. It is important to note that this band stretch is not consistent with the stretching bands of either acetic anhydride (1755 cm⁻¹) or acetic acid (1714 cm⁻¹),⁸¹ suggesting the amide bonds have formed. The ¹³C CP-MAS NMR spectrum of **Amide MOP** showed the appearance of two new peaks at 170 ppm and 22 ppm, which correspond to the incorporation of carbonyl and acetamide methyl carbons respectively, into the structure.

As expected, gas adsorption experiments of **Amide MOP** showed minimal surface area and nitrogen uptake (Figure 3-8), as the network did not regain permanent microporosity. However, thermogravimetric analysis did show that **Amide MOP** was able to swell to uptake solvents much like **Reduced MOP**, with a corresponding mass loss of 7% (Figure 3-9).

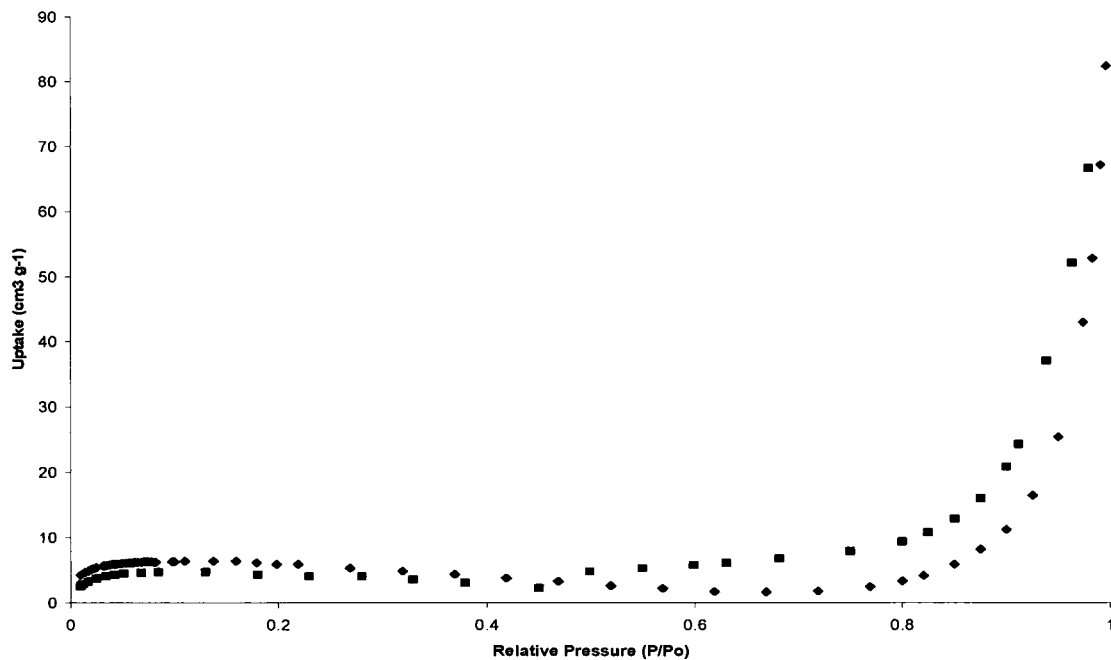


Figure 3-8. Nitrogen adsorption isotherm for **Amide MOP** (blue trace – adsorption, pink trace – desorption) measured at 77 K.

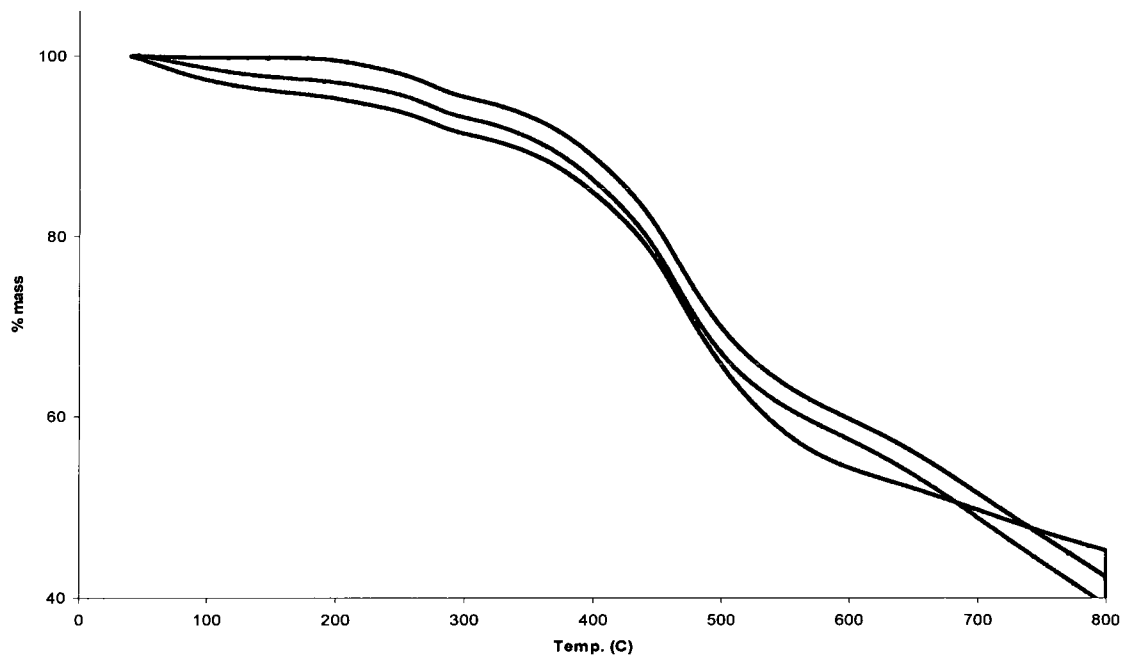


Figure 3-9. TGA traces of **Amide MOP** with THF (blue line), activated (pink line), and resoluted with THF (green line).

In addition to showing that **Amide MOP** still contains pores capable of guest exchange the smaller mass loss between the TGA of **Reduced MOP** and **Amide MOP** also suggest that the pore size within the network has been decreased. This was expected as some area within the pores is now being filled with the acetyl groups of the amide. Additionally, the solvated and resolvated TGA traces do not show identical mass losses suggesting that there could be some degradation within the network.

3.5 Summary

In summary, the first post synthetic modifications to a microporous organic network have been demonstrated. **Reduced MOP**, from the reduction of **Imine MOP**, loses its permanent microporosity. This is presumably because the rigid imine double bond has been reduced to a single bond rendering the framework more flexible and thus is allowed to collapse upon removal of guest molecules. However, **Reduced MOP** shows enhanced resistance to hydrolysis, retains high thermal stability and the ability to uptake guest molecules. Additionally, it was shown that further post synthetic modifications are possible, suggesting this research could ultimately provide a route to more chemically robust microporous organic frameworks with controlled properties, providing potential applications in gas storage, heterogeneous catalysis and molecular separations.

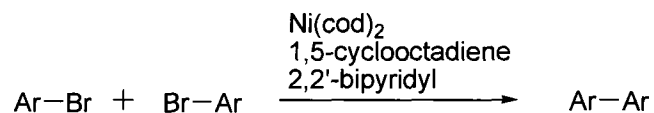
Chapter 4: Synthesis and PSM to Porous Aromatic Frameworks (PAFs)

4.1 Introduction of Tetraphenylmethane based PAFs

Porous aromatic frameworks are microporous organic polymers that are linked together by strong C-C bonds between aromatic groups that are usually formed by metal catalyzed reactions.^{9,10} PAFs, being formed by these strong C-C bonds are more robust than other MOPs such as boronate and imine networks which are susceptible to hydrolysis. Furthermore, the aromatic groups present could possibly undergo electrophilic aromatic substitution. Therefore, these materials are potentially well suited to post synthetic modifications.

When a report by Zhu. *et. al.* described a PAF based on the Yamamoto coupling of tetraphenylmethane units with a BET surface area of $5600 \text{ m}^2\text{g}^{-1}$, surpassing all other microporous materials,¹⁰ our interests were sparked to attempt the synthesis of novel PAFs. Yamamoto couplings are Ni(0) mediated reactions which link aryl bromides together as shown in Scheme 4-1. The name porous aromatic framework refers to the linking together of aromatic groups in order to form a network.

Scheme 4-1: General representation of a Yamamoto coupling.



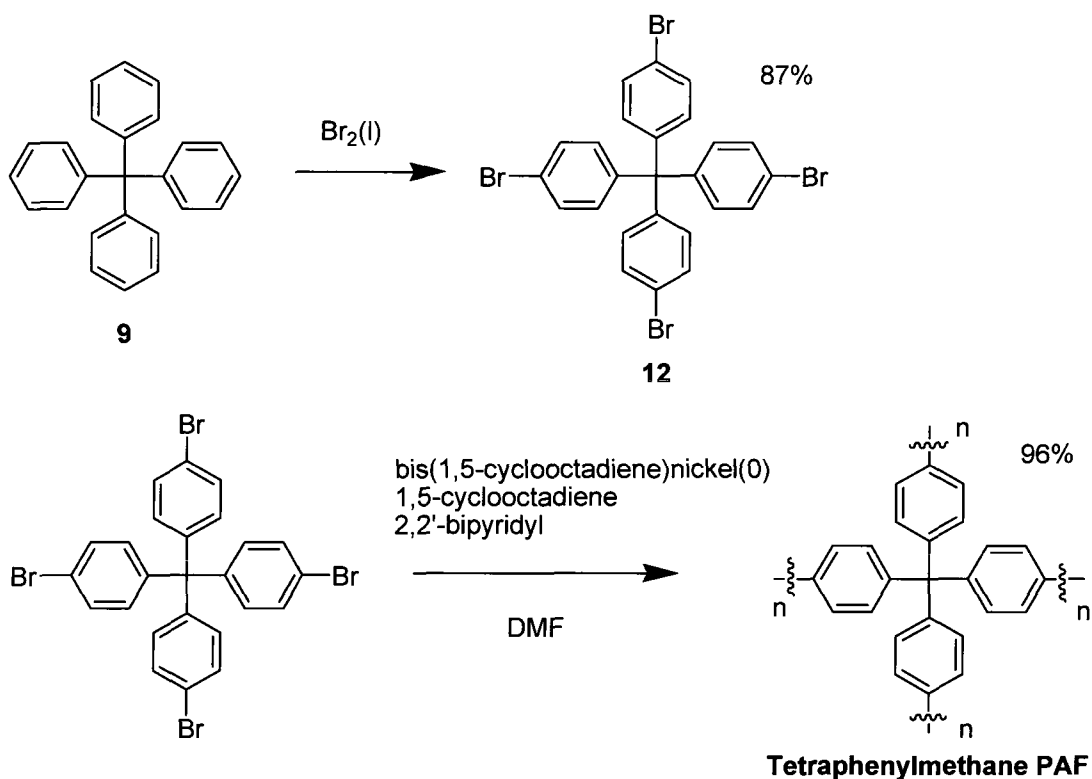
Within this chapter I will describe the repeated synthesis of PAF-1 by Zhu and coworkers as well as the post synthetic modifications made to this network. In addition to

this, I will also describe the synthesis and characterization of a novel tetra(phenyl)bimesityl based PAF.

4.2 Synthesis and Characterization of Tetraphenylmethane based PAFs

We began by repeating the PAF formation of Zhu *et. al.*, which employed Yamamoto coupling, in order to test the feasibility of following this method to create a novel PAF.

Scheme 4-2: Synthesis of Tetraphenylmethane PAF (Zhu *et. al.* PAF-1)



Tetraphenylmethane was stirred in neat $\text{Br}_2(l)$ to yield tertakis(4-bromophenyl)methane (**12**) in 87% yield.⁸² **12** was then subjected to Yamamoto coupling conditions in order to

yield **Tetraphenylmethane PAF** in 96% yield (Scheme 4-2).¹⁰ Unlike compound **12**, **Tetraphenylmethane PAF** was insoluble in THF and CHCl₃ suggesting that the network had successfully formed. In addition to this, elemental analysis and IR spectroscopy were used in order to confirm the formation of the network. Elemental analysis of starting material **12** showed a composition of C: 47.34%, H: 2.64%, Br: 50.00%, while **Tetraphenylmethane PAF** showed a composition of C: 85.56%, H: 5.37%, Br: 6.64%. A complete conversion from **12** to **Tetraphenylmethane PAF** would have resulted in a composition of C: 94.94%, H: 5.06% which was in fact reported by Zhu *et. al.* This result suggests our network has formed with a high degree of, although incomplete, conversion. These results are also supported by IR spectroscopy, which is consistent with the findings of Zhu *et. al.* (Figure 4-1).

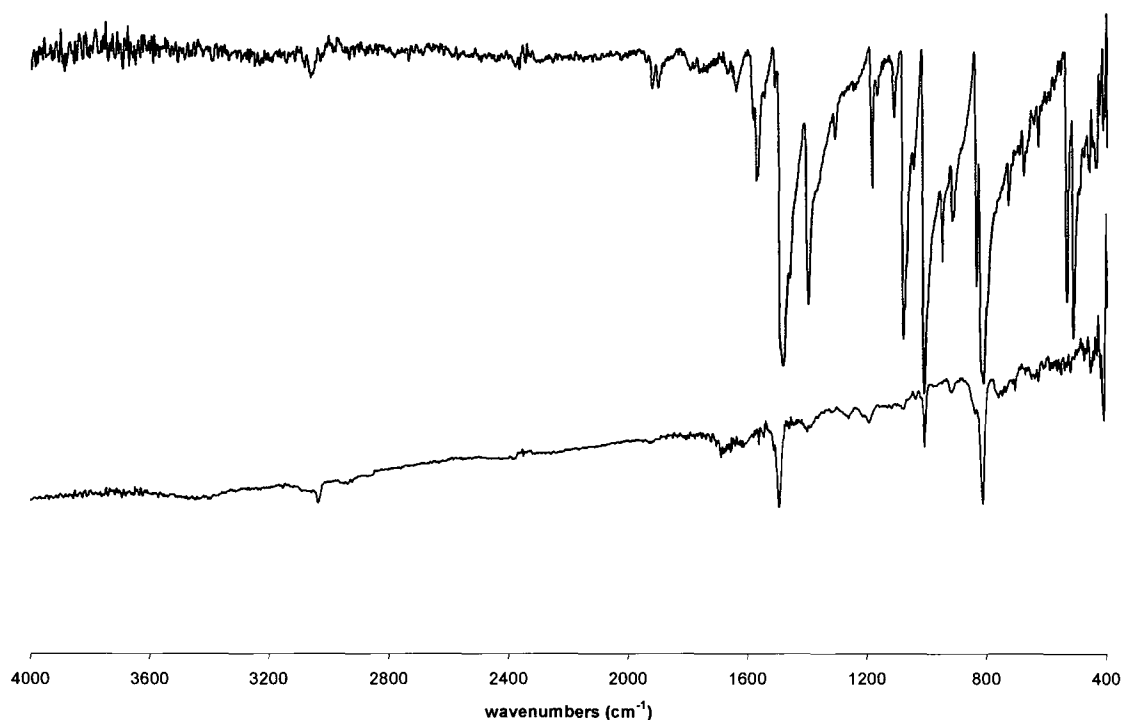


Figure 4-1: IR spectrum of **Tetraphenylmethane PAF** (pink) and tetra(4-bromophenyl)methane **12** starting material (blue).

As found by Zhu and co-workers,¹⁰ and also observed in our studies, there are characteristic bands corresponding to an Ar-Br stretch at 532 cm^{-1} and 510 cm^{-1} present in the tetrakis(4-bromophenyl)methane starting material that are no longer present in **Tetraphenylmethane PAF** lending further proof to the loss of bromine molecules and the successful formation of the framework.

Gas adsorption experiments were then performed on **Tetraphenylmethane PAF** (Figure 4-2) and a BET surface area of $2250\text{ m}^2\text{g}^{-1}$ was obtained. While this value is not nearly as high as the one reported by Zhu and coworkers of $5600\text{ m}^2\text{g}^{-1}$, it is certainly a

noteworthy value that is comparable to many porous materials leading the field in surface areas.

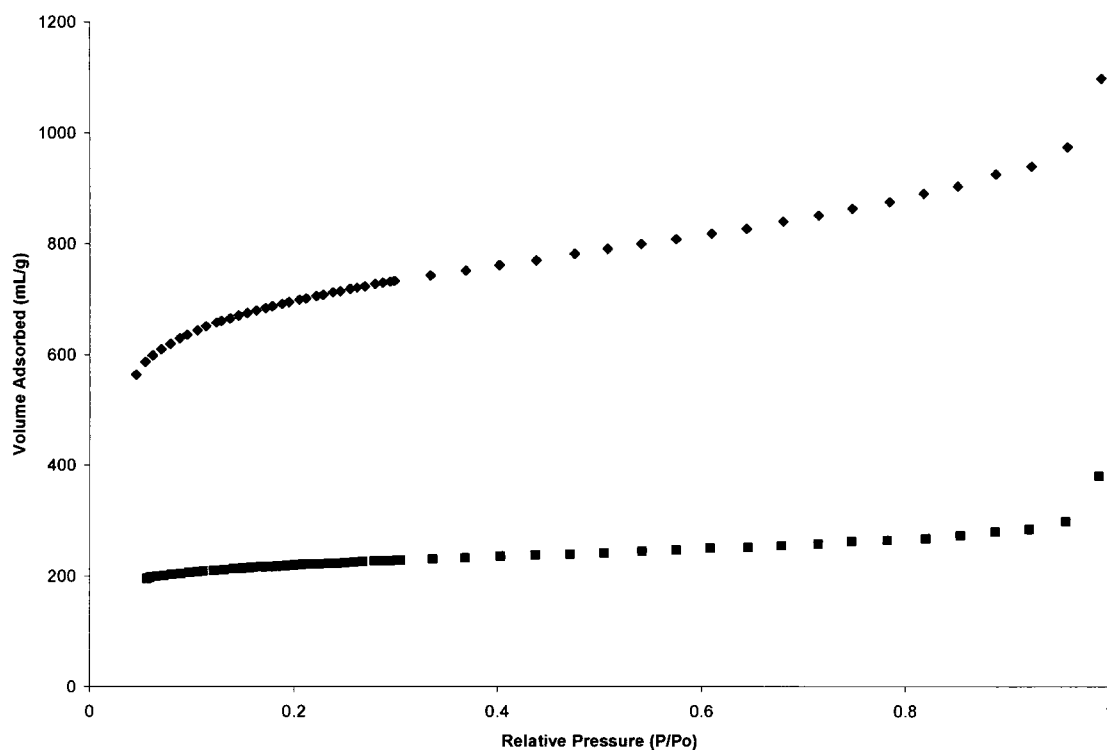
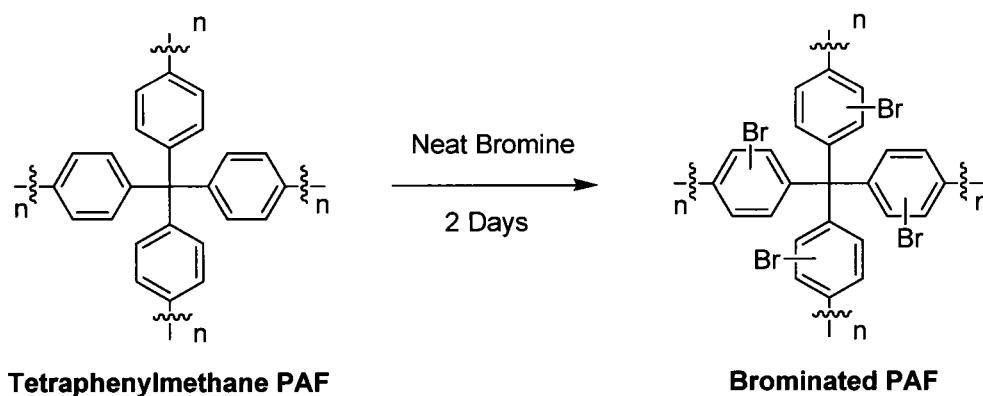


Figure 4-2: Nitrogen gas adsorption isotherm measured at 77 K of **Tetraphenylmethane PAF** (blue diamonds) and **Brominated PAF** (pink squares).

Having successfully created **Tetraphenylmethane PAF**, this material was treated with neat bromine in the hopes of brominating the aromatic rings within the network (Scheme 4-3). Our objective was to show that PSMs were possible to this network and we suspected that by bonding bromine to the aromatic groups within the network we could reduce the pore size and surface area.

Scheme 4-3: Bromination of Tetraphenylmethane PAF



After collecting and thoroughly washing **Brominated PAF** with DCM, it was placed under vacuum and heated at 100 °C in order to remove all guests from within the pores. Elemental analysis showed a chemical composition of C: 44.39%, H: 2.09%, and Br: 52.27%. This percentage of bromine corresponds to approximately one bromine atom per aromatic ring present within the network suggesting that electrophilic aromatic substitution has occurred once on each phenyl unit. Several changes in the IR spectrum also suggest that PSMs did occur to the original network (Figure 4-3).

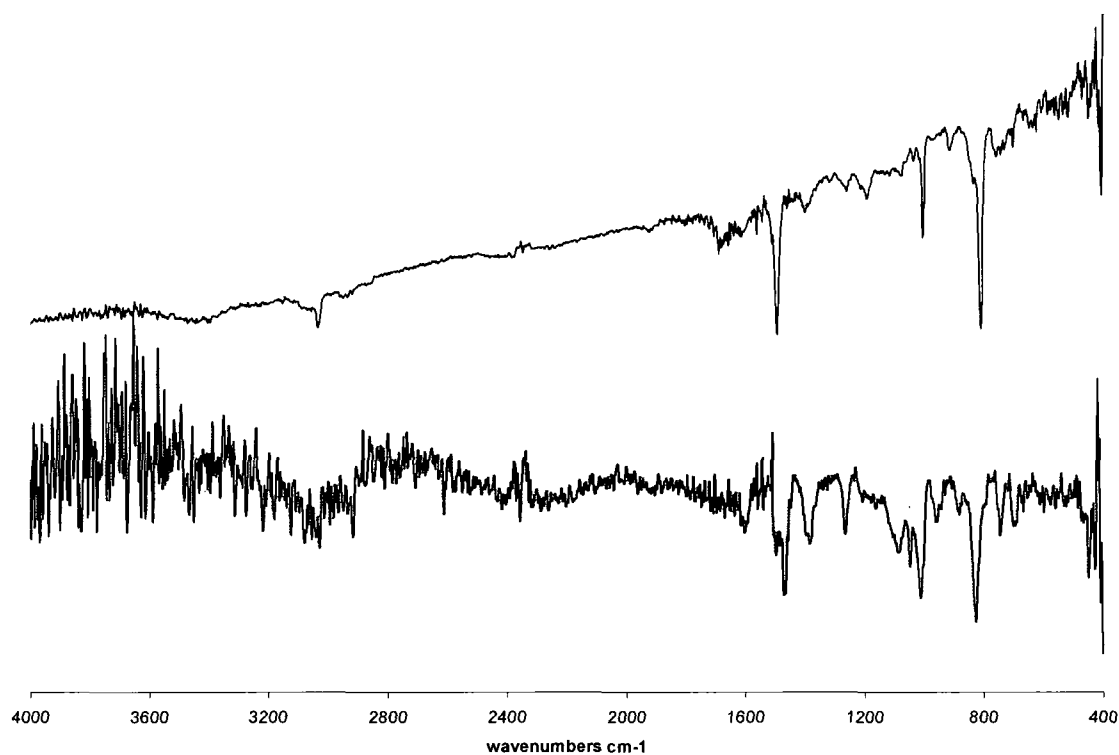


Figure 4-3: IR spectrum of **Tetrphenylmethane PAF** (pink) and **Brominated PAF** (blue).

In the newly created **Brominated PAF**, we observe several new strong absorption bands appearing including ones at 1378 cm^{-1} , 1261 cm^{-1} , 1080 cm^{-1} and 1045 cm^{-1} suggesting a definite change from the original network.

4.2 Discussion of Tetrphenylmethane based PAFs

Nitrogen gas adsorption experiments of both materials showed a large uptake of nitrogen at very low relative pressures indicating both PAFs are microporous materials. **Brominated PAF** showed an isotherm with less nitrogen uptake than that of **Tetrphenylmethane PAF** (Figure 19) and a corresponding lower BET surface area of

694 m²g⁻¹. In addition to gas adsorption analysis, investigations by TGA of the two networks were used as a measure for comparison. The TGAs show that **Tetraphenylmethane PAF** is thermally stable up to 400 °C and **Brominated PAF** shows some slight degradation after 250 °C. While **Tetraphenylmethane PAF** shows a mass loss of 28% with THF guest exchange, **Brominated PAF** only shows a mass loss of 16% under the same conditions (Figure 4-4).

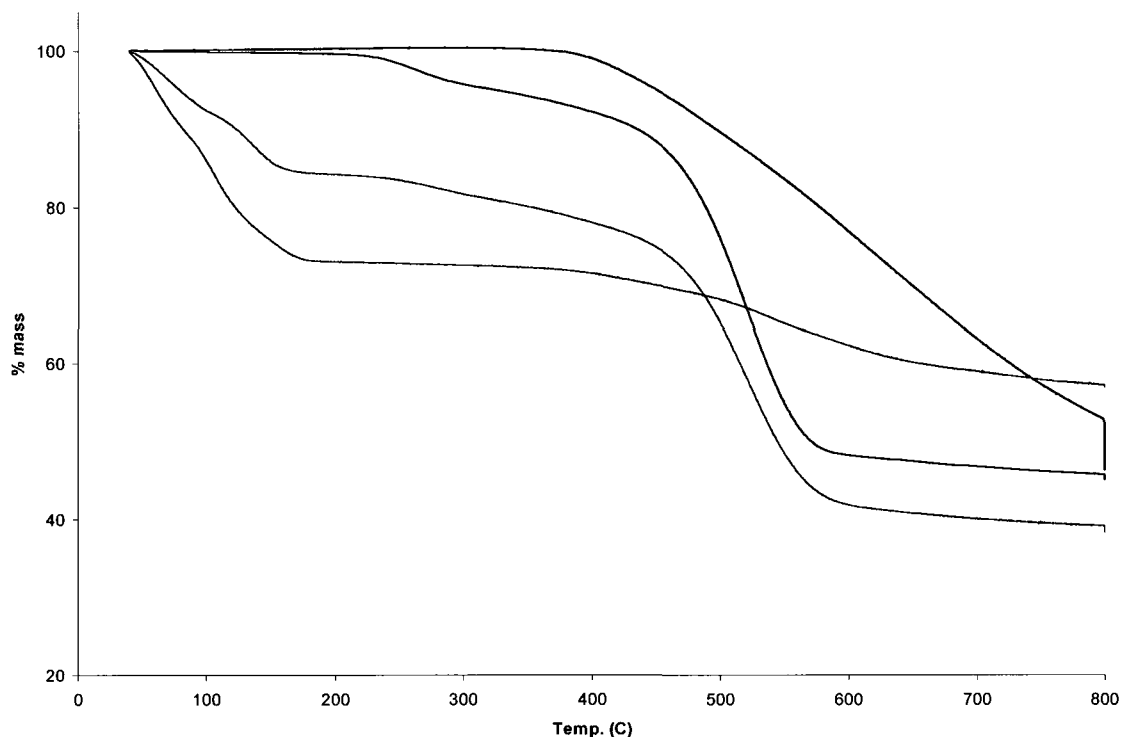


Figure 4-4: TGA trace of **Tetraphenylmethane PAF** activated (dark green)/THF guest (light green) and **Brominated PAF** activated (dark blue)/THF guest (light blue).

These results support our original hypothesis that it is possible to post synthetically modify a microporous organic framework via bromination of the aromatic groups present, effectively reduced the pore size within the network. One drawback of this

system is that the pore size and surface area of the network is significantly reduced, which would possibly limit its use in applications. It is therefore of interest to attempt to create a PAF with larger pore sizes and channels to which added functionality would not decrease surface areas and pore sizes to such a large degree.

4.3 Bimesityl PAF Introduction

Having successfully demonstrated that the Yamamoto coupling performed by Zhu and coworkers is a feasible approach to creating extended microporous organic networks and performing PSMs to **Tetraphenylmethane PAF** we then turned our attention to the synthesis of a novel PAF.

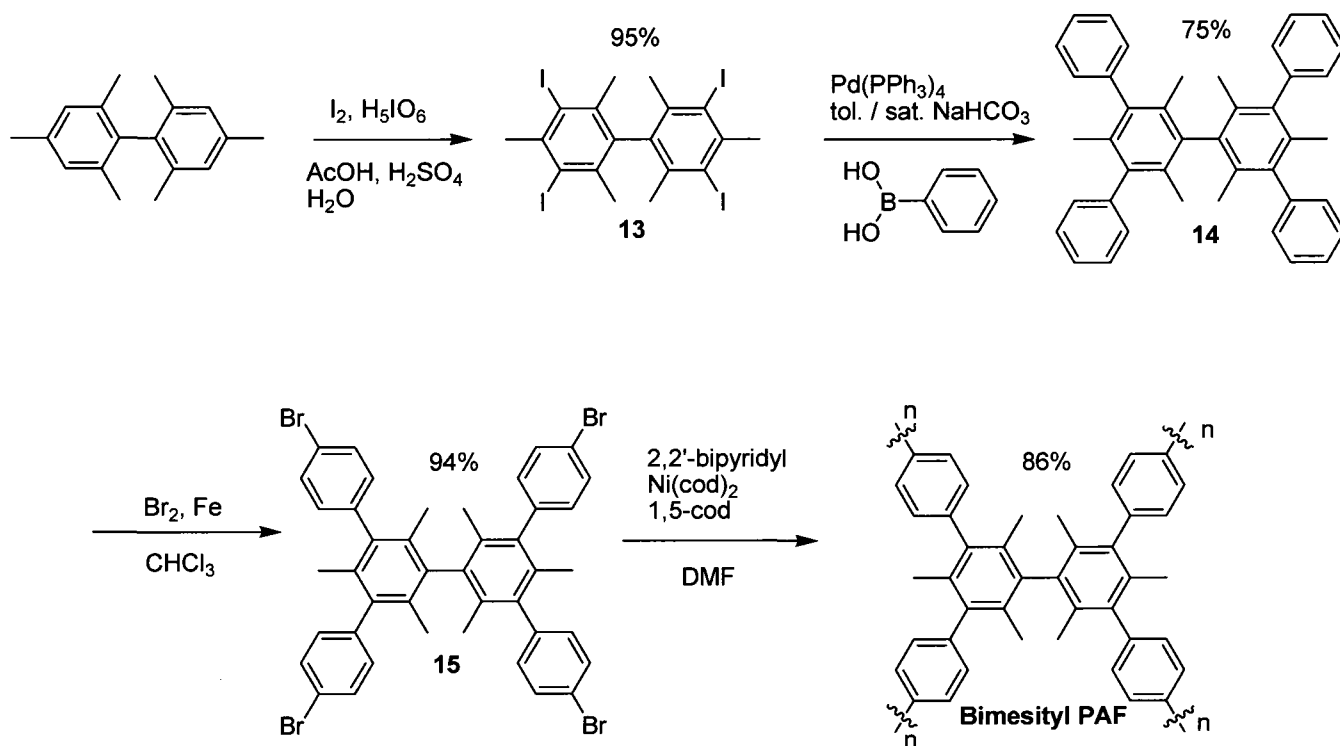
We chose a tetraphenylbimesityl core due to the geometry of the molecule. The two central phenyl rings are perpendicular to one another and thus a network formed from this material will extend in a 3D manner, exhibiting free volume between subunits. The bimesityl core also has accessible methyl groups which could potentially be used for post synthetic modifications should we choose to follow this line of research in the future.

4.4 Synthesis of Bimesityl PAF

In order to synthesize the tetrakis(4-bromophenyl)bimesityl monomer (**15**), bimesityl, which was previously prepared by K. Maly according the procedure of Fischer *et. al.*,⁸⁴ was first iodinated in the presence of $I_{2(s)}$ and H_5IO_6 while stirring an $AcOH/H_2SO_4$ mixture yielding 3,3',5,5'-tetraiodobimesityl (**13**) in 95%.⁸⁵ **13** was

subsequently reacted with phenylboronic acid under Suzuki conditions in order to yield tetraphenylbimesityl (**14**) in 75% yield.⁸⁵ The four phenyl rings of **14** were then brominated, each in the para position, using Br_{2(l)} in the presence of Fe powder acting as a catalyst.⁸⁵ This yielded the desired building block, tetrakis(4-bromophenyl)bimesityl **15**, in 94% (Scheme 4-4).

Scheme 4-4: Synthesis of Bimesityl PAF.



Compound **15** was subjected to Yamamoto conditions in a nitrogen glove box in order to form the novel **Bimesityl PAF** which washed thoroughly with THF, H_2O , and $CHCl_3$ in order to remove any impurities.

4.5 Characterization of Bimesityl PAF

Similar to the characterization of **Tetraphenylmethane PAF**, IR spectroscopy and elemental analysis were used for the characterization of **Brominated PAF**. Elemental analysis of the starting material, tetrakis(4-bromophenyl)bimesityl, provided a chemical composition of C: 58.60%, H: 4.17%, and Br: 37.29%, while **Bimesityl PAF** showed a chemical composition of C: 81.41%, H: 6.02%, and Br: 7.48%. Assuming complete conversion of **15** to **Bimesityl PAF**, the theoretical chemical composition would be C: 93.63%, H: 6.37% which suggests a near complete conversion during the Yamamoto coupling. This result is further confirmed by comparing the IR spectra of both the starting material and network product (Figure 4-5). There is a clear disappearance of the Ar-Br in the spectrum of **Bimesityl PAF** which is observed at 515 cm^{-1} in the spectrum of **15** suggesting most of the bromines have reacted and the network has formed.

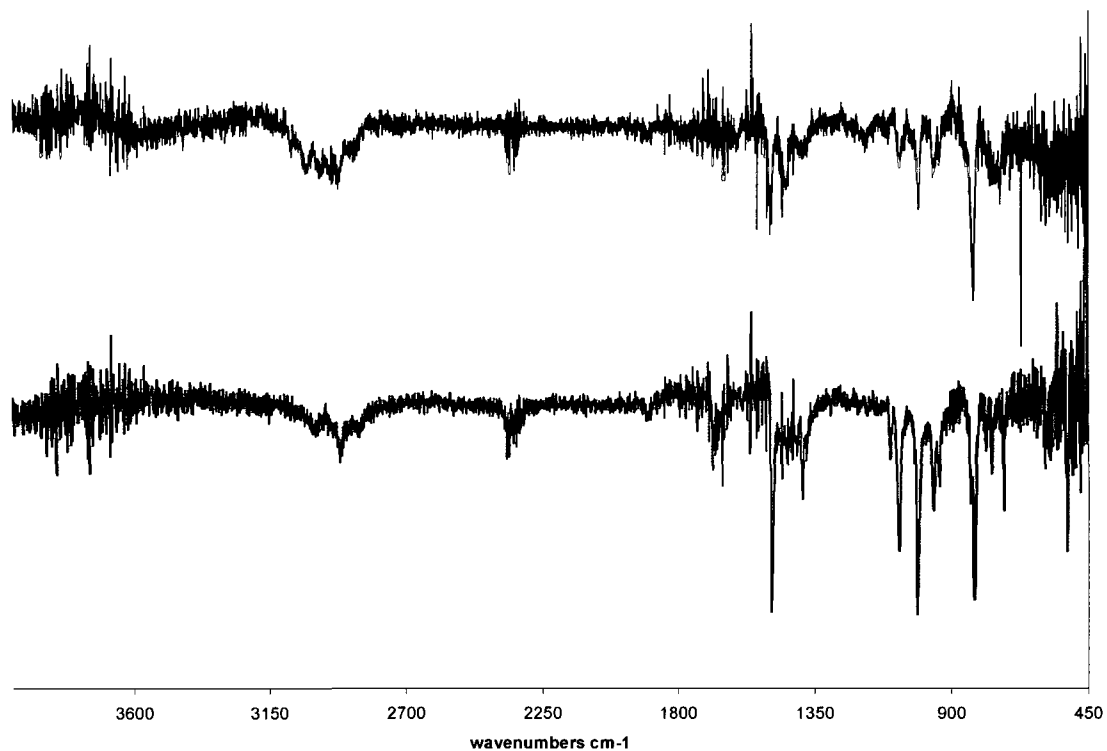


Figure 4-5: IR spectrum of tetrakis(4-bromophenyl)bimesityl, **15**, starting material (blue) and **Bimesityl PAF** (pink).

After successfully creating a novel network, our attention was turned to testing the surface area and uptake through nitrogen gas adsorption.

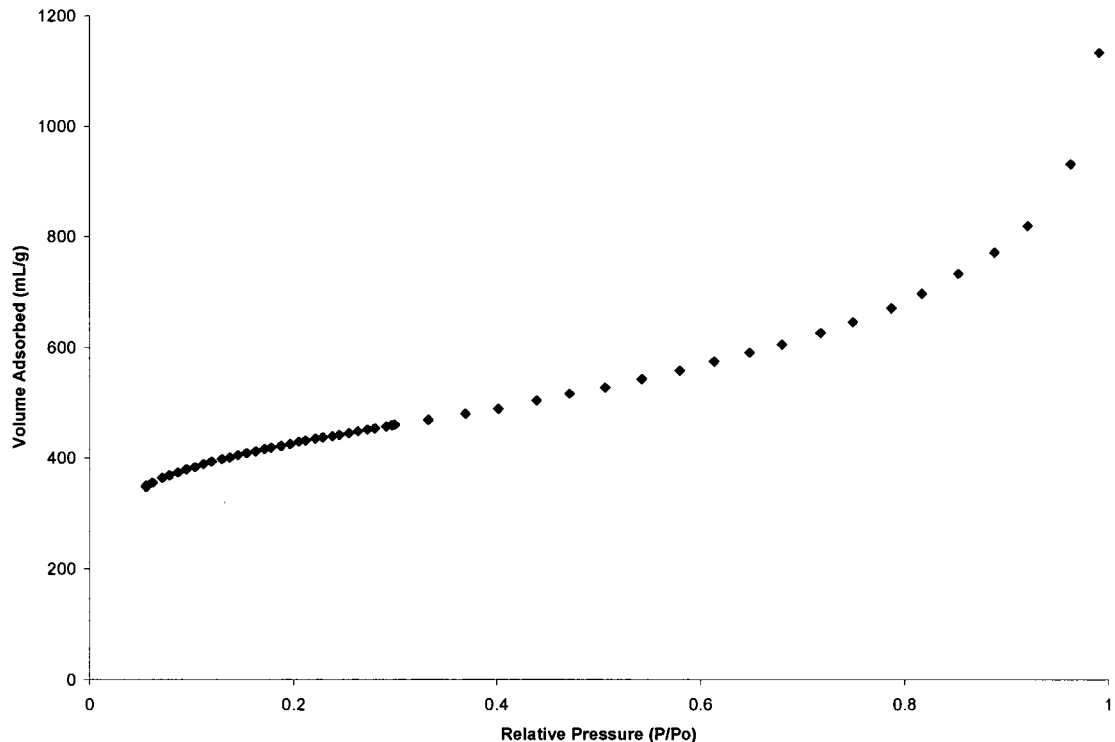


Figure 4-6: Nitrogen gas adsorption isotherm measured at 77 K for **Bimesityl PAF**.

As shown in Figure 4-6, there was significant nitrogen uptake at very low relative pressures, characteristic of microporous materials. In addition to this, a large BET surface area of $1424 \text{ m}^2 \text{ g}^{-1}$ was obtained from the experiment. While this surface area is not as high as the highest recorded microporous materials to date, it is still relatively large and in the range of other microporous materials.

TGA analysis on **Bimesityl PAF** was also performed in order to test the networks solvent uptake capacities. Figure 4-7 shows a THF solvent uptake of 18% by mass for **Bimesityl PAF** after being activated. In addition to showing the solvent uptake capacity of the material, the TGA trace also tells us that **Bimesityl PAF** is thermally stable for temperatures up to 400 °C.

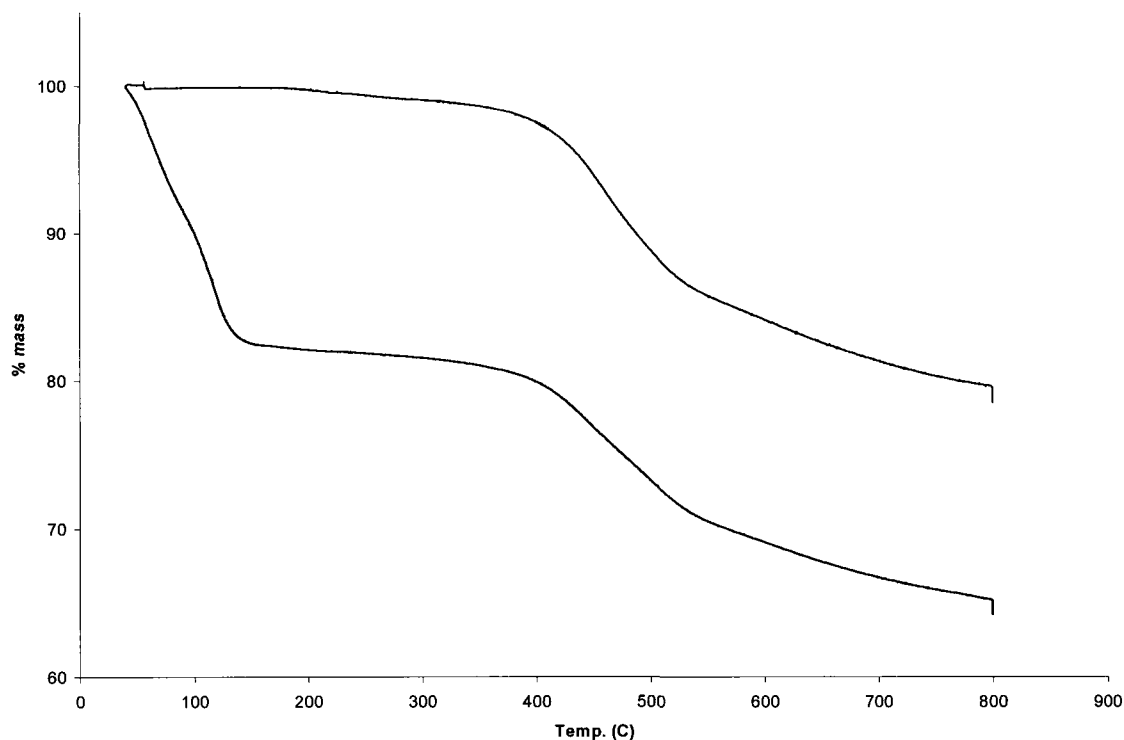


Figure 4-7: TGA trace of **Bimesityl PAF** activated (pink) and **Bimesityl PAF** THF guest (blue).

4.6 Summary

In summary we have created a tetraphenylmethane-based PAF which we were able to brominate via electrophilic aromatic substitution, reducing the surface area from $2250 \text{ m}^2\text{g}^{-1}$ to $694 \text{ m}^2\text{g}^{-1}$ and the solvent uptake capacity 12% by mass, effectively reducing the pore size within the network.

In addition to this, we were able to create a novel PAF based on a tetraphenylbimesityl monomer which showed significant surface area of $1424 \text{ m}^2\text{g}^{-1}$, solvent uptake capacities of 18% by mass and was thermally stable at temperature up to $400 \text{ }^\circ\text{C}$.

Chapter 5: Conclusions and Future Work

As described in Chapter 2, a permanently microporous, novel triptycene based MOP was synthesized which showed relatively high thermal stability up to 400 °C and guest uptake of up to 19 %. However, the relatively low surface area obtained ($200 \text{ m}^2\text{g}^{-1}$) coupled with the low chemical stability of B-O based linkers used for this network led to no further research in these specific methods.

From Chapter 3, I was successfully able to perform the first post synthetic modifications to a purely organic microporous network. It was found that the reduction to an imine based network adds chemical stability to the network as it is no longer susceptible to hydrolysis, however, the rigidity imparted by the imine bonds is lost along with permanent microporosity. The network does remain porous and is able to swell to uptake solvent guest molecules 18% by mass. Further post synthetic modifications were then possible by acetylating the amines within the network and reducing the pore size as solvent uptake capacities are reduced to 11% by mass.

As laid out in Chapter 4, I created a novel porous aromatic framework via a Yamamoto coupling using a tetraphenylbimesityl core which showed an impressive BET surface area of $1424 \text{ m}^2\text{g}^{-1}$. The network was also able to uptake 18% by mass of guest solvent as shown by TGA. In addition to this, I was able to reproduce a tetraphenylmethane based PAF of Zhu *et. al.* and perform an electrophilic aromatic substitution to this network. This modification reduced the uptake volume of the network from 28 % by mass to 16 % by mass, and reduced the BET surface area from $2250 \text{ m}^2\text{g}^{-1}$ to $694 \text{ m}^2\text{g}^{-1}$.

As an overall thesis I have explored both the novel synthesis of new microporous organic polymers as well as exploring the first documented post synthetic modifications to purely organic networks.

These studies can be applied and further extended into future work. It would be of interest to attempt to improve the original imine network formation described by Yaghi in Chapter 3. The material we were able to synthesize, while showing permanent microporosity, was not a well ordered Covalent Organic Framework. Thus, it would be interesting to be able to perform the first post synthetic modifications to a COF and observe the results and feasibility.

It is also of interest to explore further post synthetic modifications to the **Bimesityl PAF** through benzylic bromination to the accessible methyl groups present. It is our hope that we would be able to functionalize the network while not significantly affecting the overall surface area of the network. This would allow the material to remain a viable option for applications while being suitable for tailoring.

Chapter 6: Experimental

6.1 General

6.1.1 Infrared Spectroscopy

Infrared Spectra were recorded as KBr disks using a Perkin Elmer Spectrum BX FT-IR Spectrometer. KBr pellets were pressed under atmospheric conditions. A blank KBr pellet was always pressed and subtracted from the spectrum of the sample.

6.1.2 NMR Spectroscopy

^1H and ^{13}C spectra were recorded on a Varian 300 MHz (^1H) Unity Inova NMR Spectrometer in the indicated solvent. Chemical shifts are reported in δ scale downfield from the peak for tetramethylsilane.

6.1.3 Elemental Analysis

All elemental analysis experiments were performed by Midwest Microlabs, LCC, Indianapolis, IN.

6.1.4 Carbon-13 CP/MAS NMR spectroscopy

All experiments were kindly performed by Professor David Bryce at the University of Ottawa. Samples were ground into fine powders and packed into 4 mm o.d. zirconia

rotors. NMR spectra were acquired with high-power proton decoupling at 9.4 T ($\nu_0(^{13}\text{C}) = 100.6$ MHz) using a Bruker Avance III console and a 4 mm triple-resonance Bruker MAS NMR probe. The magic angle was set by maximizing the number of rotational echoes in a ^{79}Br MAS NMR experiment on powdered KBr. Carbon-13 CP/MAS NMR pulse calibrations and chemical shift referencing were performed using adamantane ($\delta = 38.55$ ppm for the high-frequency peak, relative to the primary standard TMS). Ninety degree ^1H pulse widths were 3.45 μs , contact pulses were 1.5 or 2.0 ms, acquisition times were 40-50 ms, and recycle delays were 20-50 s. Approximately 1 k to 2 k scans were averaged for each of the COF samples. MAS rates were chosen to eliminate the overlap of spinning sidebands with resonances of interest, and ranged from 11111 to 13600 Hz. FIDs were processed with zero-filling, 15-20 Hz exponential apodization, and Fourier transformation.

6.1.5 Gas Adsorption Studies

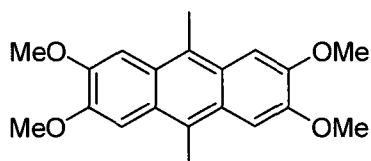
Gas adsorption isotherms were measured volumetrically using a Quantachrome NOVA 2200e surface area and pore size analyzer or a Micromeritics ASAP 2010 automated adsorption analyzer. Samples were degassed at 120 °C for 12 hours prior to measurement. A liquid nitrogen bath (77 K) was used for N_2 isotherm. The N_2 gases used were UHP grade. Brunauer-Elmett-Teller (BET) was used to determine the specific surface areas ($A_{\text{BET}}, \text{m}^2 \text{g}^{-1}$) using the adsorption data over 0.05 – 0.30 P/Po.

6.1.6 Thermogravimetric Analysis

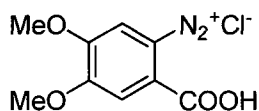
Thermogravimetric analysis was conducted using a TA Instruments Q-50 series thermal gravimetric analyzer with samples held in a platinum pan under nitrogen. A heating rate of 10 K min⁻¹ was used.

6.2 Synthesis

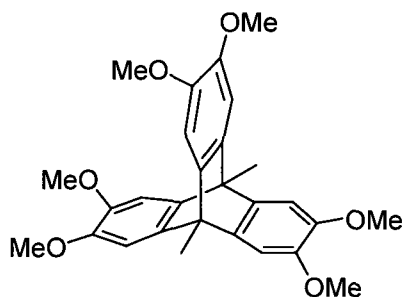
All starting materials and solvents were obtained from commercial sources and used without purification, unless otherwise specified. Anhydrous and oxygen-free solvents were dispensed from a custom-built solvent purification system which used purification columns packed with activated alumina and supported copper catalyst (Glasscontour, Irvine, CA).



9,10-Dimethyl-2,3,6,7-tetramethoxyanthracene (1).⁷⁷ A mixture of veratrole (3.2 mL, 0.025 mol), acetaldehyde (1.4 mL, 0.025 mol) and acetonitrile (1.31 mL, 0.025 mol) were added dropwise at 0 °C slowly over 15 minutes to a conc. H₂SO₄ (12.5 ml). The reaction mixture was allowed to stir for 30 minutes and then poured slowly over ice water (2 x 250 ml). The precipitate that formed was filtered, allowed to air dry overnight, and recrystallized from chloroform to yield **1** as yellow crystals (3.22 g, 79%). ¹H NMR (300 MHz, CDCl₃) δ 7.42 (s, 4H), δ 4.09 (s, 12H), δ 2.96 (s, 6H); ¹³C NMR (75 MHz, CDCl₃) δ 149.0, 126.0, 124.1, 102.9, 55.9, 15.0.



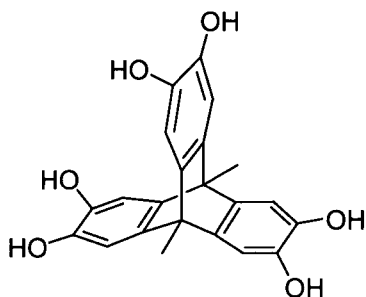
4,5-Dimethoxybenzenediazonium-2-carboxylate (2).⁷⁸ To a vigorously stirred solution of 2-amino-4,5-dimethoxybenzoic acid (6 g, 0.0347 mol) in ethanol (180 mL) at 0 °C was added conc. HCl dropwise. Solution thickened and required stirring by hand in order to loosen the material as isoamyl nitrite (7.00 mL, 0.0521 mol) was added dropwise. The thick solution loosened and was allowed to stir for 15 minutes. Ether (180 mL) was added to dilute the solution and was allowed to stir another 30 minutes. The resulting precipitate was filtered, washed with ether and allowed to dry yielding **2** as a beige solid (7.81 g, 92 %).



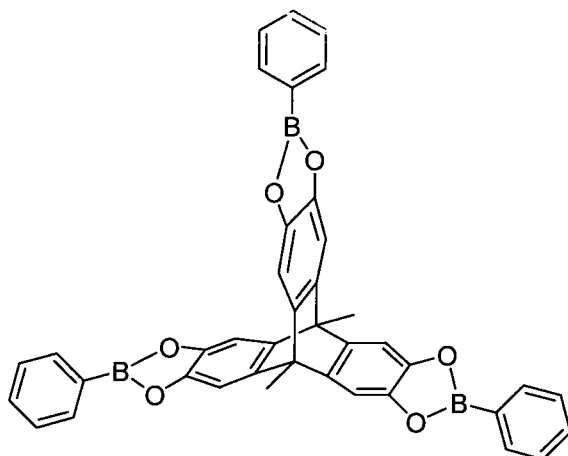
9,10-Dimethyl-2,3,6,7,14,15-hexamethoxy-9,10-[1',2']benzenoanthracene (3).⁷⁸

Degassed propylene oxide (45 ml) was added to a mixture of **1** (2.15 g, 6.58 mmol) and **2** (7.00 g, 28.62 mmol) suspended in degassed dichloroethane (200 ml) and heated at reflux for 36 hours. Solution was cooled to room temperature and concentrated under reduced pressure. Solid was then suspended in acetone and filtered to obtain a mixture of **1** and product. This mixture was recrystallized in DCM causing unreacted **1** to crystallize, which was removed by filtration. The solution of product in DCM was concentrated

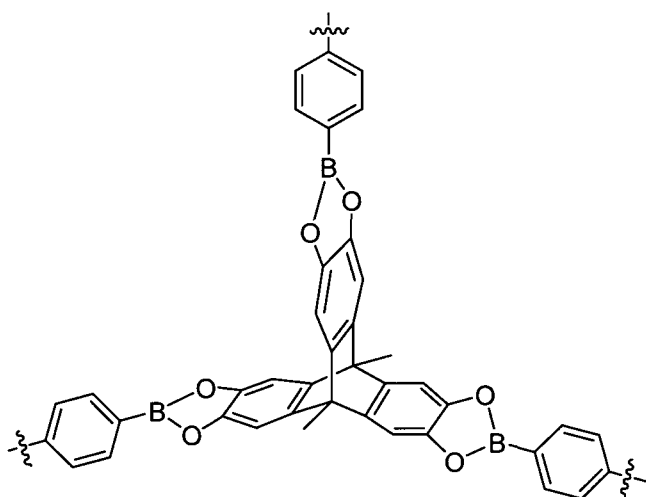
under reduced pressure and then dried under vacuum to obtain **3** as a white solid (1.41 g, 57 %). ^1H NMR (300 MHz, CDCl_3) δ 6.93 (s, 6H), δ 3.84 (s, 18H), δ 2.38(s, 6H); ^{13}C NMR (75 MHz, CDCl_3) δ 145.6, 142.0, 105.8, 56.4, 47.7, 14.0.



9,10-Dimethyl-2,3,6,7,14,15-hexahydroxy-9,10-[1',2']benzenoanthracene (4).⁷⁸ 1 M BBr_3 (4 mL, 3.09 mmol) in DCM was added an oven dried flask containing a stirred solution of **3** (0.20 g, 0.42 mmol) in anhydrous DCM. The mixture was allowed to stir for 4 hours and then poured over ice water to form a pink precipitate after stirring for 30 minutes. The precipitate was filtered, collected and dried under $\text{N}_2(\text{g})$ to yield **4** as a pink solid (0.16 g, 100 %). ^1H NMR (300 MHz, $\text{DMSO-}d_6$) δ 8.43 (s, 6H), δ 6.64 (s, 6H), δ 1.99 (s, 6H); ^{13}C NMR (75 MHz, $\text{DMSO-}d_6$) δ 140.53, 140.46, 108.8, 45.9, 13.7.

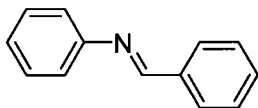


Triptycene Tris-phenylboronate (5). To an oven dried flask was added **4** (70 mg, 0.19 mmol) and phenylboronic acid (66 mg, 0.57 mmol) which was then purged with $N_{2(g)}$ for 15 minutes. A mixture of anhydrous THF (10 mL): MeOH (0.2 mL) were then added to the flask to solvate the solids. The mixture was refluxed for 36 hours at which point an equivalent amount of the solvent mixture was added to prevent the reaction from going dry. The solution was then allowed to reflux for an additional 36 hours. The precipitate that formed was filtered and washed with CH_3CN to yield **5** (66 mg, 50 %). 1H NMR (300 MHz, $DMSO-d_6$) δ 8.03 (s, 6H), δ 7.77 (d, 6H), δ 7.39-7.29(m, 9H), δ 1.98(s, 6H). ^{13}C NMR (75 MHz, $CDCl_3$) δ 145.7, 144.2, 135.0, 132.4, 128.4, 106.3, 48.73, 15.1.

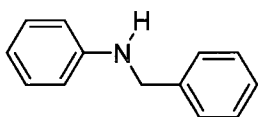


Framework 1. A pyrex glass tube measuring 6mm interior/8mm exterior in diameter was charged with **4** (19 mg, 0.05 mmol), benzenediboronic acid (25 mg, 0.15 mmol) and 1 mL of a 1:1 mesitylene:dioxane mixture. The tube contents were flash frozen in liquid nitrogen and evacuated to a pressure of 150 mtorr. The tubes were then flame sealed at a length of 12 cm and allowed to warm to room temperature. The contents were then heated at 100 °C for 72 hours. The grayish purple precipitate was then filtered and

washed with large amounts of mesitylene, dioxanes, CHCl_3 , and THF. The precipitate was collected and dried under vacuum at $100\text{ }^\circ\text{C}$ for 24 hours to evacuate the pores of all solvent guest molecules. Yield, 40 mg.



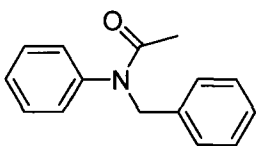
N-benzylidenebenzenamine (6). Aniline (4 g, 37.69 mmol) was added dropwise to a solution of benzaldehyde and ether. Mixture was allowed to stir for 4.5 hours and then concentrated under reduced pressure. Yellow solid was recrystallized in hexanes and collected by filtration, 5.02 g (73.6 %) ^1H NMR (300 MHz, CDCl_3) δ 7.27-7.32 (m, 3H), δ 7.43-7.49 (m, 2H), δ 7.53-7.56 (m, 3H), δ 7.96-7.99 (m, 2H), δ 8.52 (s, 1H); ^{13}C NMR (75MHz, CDCl_3) δ 121.1, 126.2, 129.0, 129.1, 129.4, 131.6, 136.4 152.3, 160.6. Spectroscopic data matches that previously reported in the literature.⁸⁰



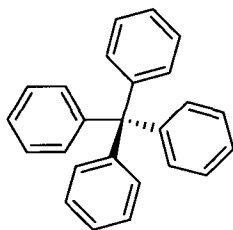
N-benzylbenzenamine (7). To a solution of N-benzylidenebenzenamine (**6**) (1.08 g, 6.0 mmol) in anhydrous THF was added 1 M borane-THF (10 ml, 10.0 mmol) dropwise. The mixture was allowed to stir for 1 hour and then quenched with water. The product was extracted with ether, dried with MgSO_4 , filtered and concentrated under reduced pressure. After being placed under vacuum overnight the liquid solidified to yield **7** (0.92 g, 85 %) as a white solid. ^1H NMR (300 MHz, CDCl_3) δ 4.36 (s, 2H), δ 6.67 (d, $J = 7.8$ Hz, 2H), δ 6.75 (t, $J = 7.2$ Hz, 1H), δ 7.21 (t, $J = 8.1$ Hz, 2H), δ 7.30-7.42 (m, 5H); ^{13}C NMR

(75MHz, CDCl₃) δ 48.7, 113.2, 117.9, 127.5, 127.8, 128.9, 129.5, 139.6, 148.3.

Spectroscopic data matches that previously reported in the literature.⁸⁰

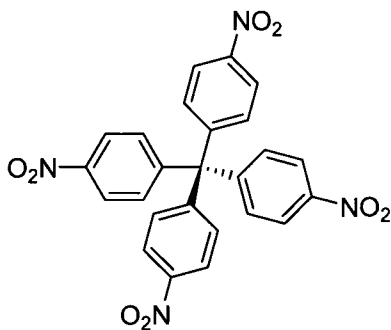


N-benzyl-N-phenylacetamide (8). N-benzylbenzenamine (**7**) (0.255 g, 1.13 mmol) was dissolved in 10 ml of Ac₂O and heated to 100 °C in a sealed pyrex tube. The solution was stirred for 2.5 hours then poured over ice water and allowed to stir for an additional 15 minutes. Product was then extracted with ether and the organic fractions were combined and washed with 1 M NaOH to remove any remaining AcOH. The organic layer was then dried with MgSO₄ and concentrated under reduced pressure to yield **8** (0.313 g, 100 %) as a clear liquid. ¹H NMR (300 MHz, CDCl₃) δ 1.86 (s, 3H), δ 4.87 (s, 2H), 6.95 (d, J = 8.1 Hz, 2H), δ 7.19-7.28 (m, 8H); ¹³C NMR (75 MHz, CDCl₃) δ 23.0, 53.0, 127.6, 128.1, 128.4, 128.6, 129.0, 129.8, 137.7, 143.1, 170.5. Spectroscopic data matches that previously reported in the literature.⁸¹



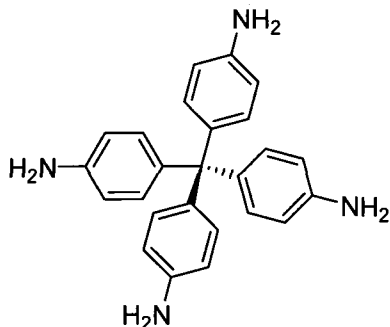
Tetraphenylmethane (9).⁸² Trityl chloride (18.52 g, 0.066 mol) and aniline (17 mL, 0.186 mol) were combined in a r.b. flask and heated at 200 °C for 5 minutes. A brown liquid formed which was cooled to 90 °C, which then solidified and 100 mL conc. HCl

was added and the mixture was refluxed for 1 hour. The mixture was cooled and a precipitate was collected via filtration. The precipitate was then dissolved in EtOH (140 mL) and conc. H₂SO₄ (20 ml), cooled to -10 °C in an acetone/ice bath and isopentyl nitrite (15 mL) was added dropwise. The mixture was stirred for 30 minutes at which point 30 mL of hypophosphorous acid was added at -10 °C. Bubbling was observed corresponding to N_{2(g)} evolving. The mixture was then heated at reflux for 30 minutes before cooling to room temperature, collecting the formed precipitate via filtration and washing with water. The resulting light beige solid was allowed to air dry for 48 hours yielding **9** (20.11 g, 95 %). ¹H NMR (300 MHz, CDCl₃) δ 7.28-7.15 (m, 20H); ¹³C NMR (75 MHz, CDCl₃) δ 147.0, 131.4, 127.7, 126.1, 18.6.

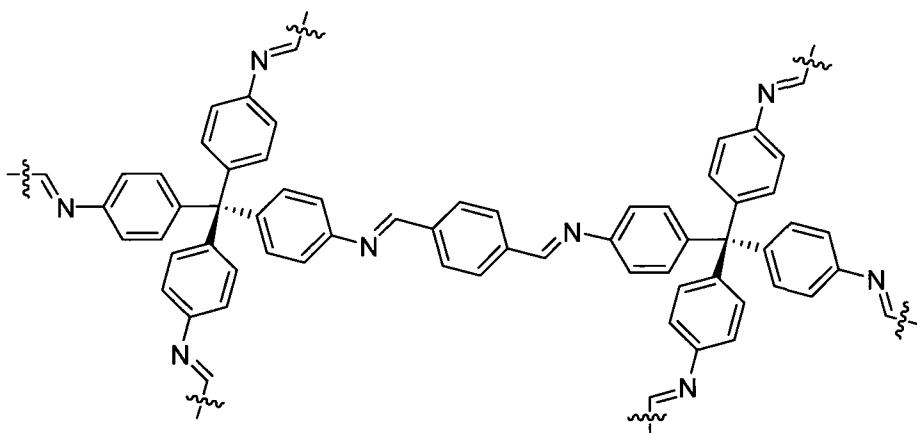


Tetrakis(4-nitrophenyl)methane (10).⁸² In small portions was added tetraphenylmethane **9** (10.0 g, 0.031 mol) to a solution of fuming HNO₃ (50 ml) at -10 °C in an acetone/ice bath. After additions were complete the mixture was allowed to stir for 1 hour. A mixture of AcOH/Ac₂O (33 mL/17 mL) was added and the solution was allowed to stir for an additional 1 hour. Glacial AcOH (100 mL) was then added to the solution and allowed to stir for an additional hour. A yellow precipitate formed that was collected via filtration and washed with AcOH and MeOH. The product was dried under

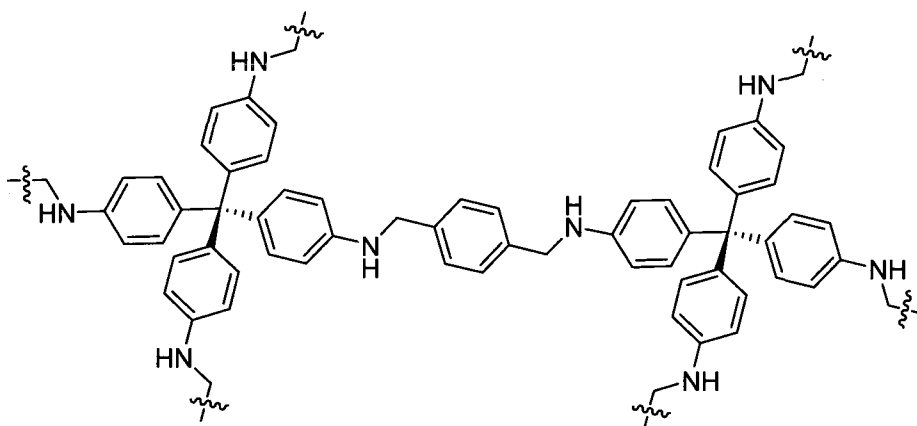
vacuum to yield 10.73 g (69 %). ^1H NMR (300 MHz, $\text{DMSO-}d_6$) δ 8.23 (d, $J = 9.3$ Hz 8H), δ 7.60 (d, $J = 8.7$ Hz, 8H) ^{13}C NMR (75 MHz, $\text{DMSO-}d_6$) δ 146.6, 136.9, 132.1, 113.6, 62.2.



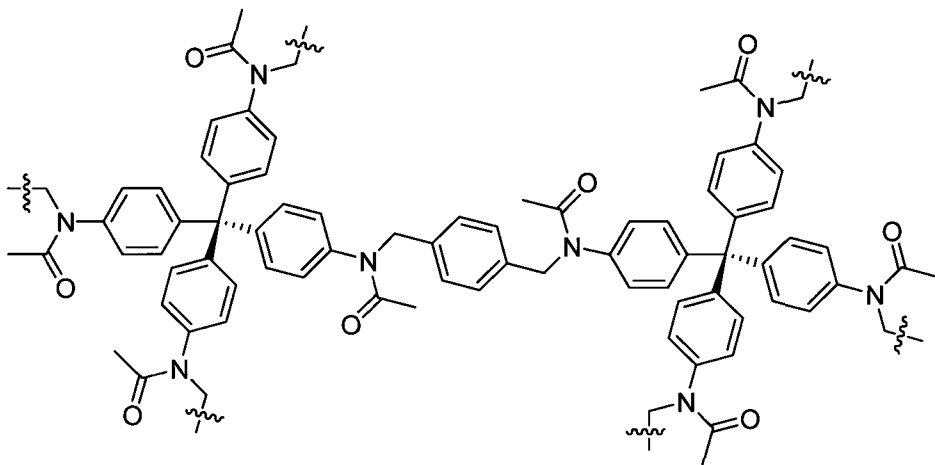
Tetrakis(4-aminophenyl)methane (11).⁸² Tetrakis(4-nitrophenyl)methane **10** (5.73 g, 11.4 mmol) anhydrous cyclohexene (100 mL) and anhydrous THF (300 mL) were combined in an oven dried flask and purged with $\text{N}_{2(g)}$ for 15 minutes. Palladium 10 wt. % on carbon powder catalyst (2 g, 1.29mmol) was added and the mixture was heated at reflux for 72 hours. The mixture was then allowed to cool and a brown precipitate was filtered, washed with MeOH and dried under $\text{N}_{2(g)}$ overnight (2.05 g, 47 %). ^1H NMR (300 MHz, $\text{DMSO-}d_6$) δ 6.65 (d, $J = 8.7$ Hz, 8H), δ 6.35 (d, $J = 8.7$ Hz, 8H) ^{13}C NMR (75 MHz, $\text{DMSO-}d_6$) δ 149.9, 145.0, 130.4, 122.7, 64.2.



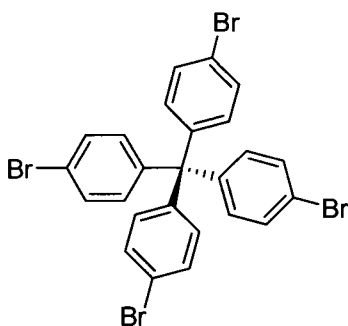
Imine MOP. A pyrex glass tube measuring 6 mm interior/8 mm exterior in diameter was charged with tetrakis(4-anilyl)methane **11** (20 mg, 0.052 mmol), terephthalaldehyde (12 mg, 0.089 mmol) and mixture of dioxane (0.8 mL) and 2 M AcOH (0.2 mL). The tube was flash frozen in liquid nitrogen, evacuated to a pressure of 150 mtorr and flame sealed at a length of 12 cm. The contents of the tube were allowed to warm to room temperature and then heated at 100 °C for 72 hours. The yellow solid formed was collected via filtration and washed with large amounts of THF. The yellow precipitate was collected and dried under vacuum at 100 °C for 24 hours to evacuate the pores of all solvent guest molecules. Yield, 48 mg.



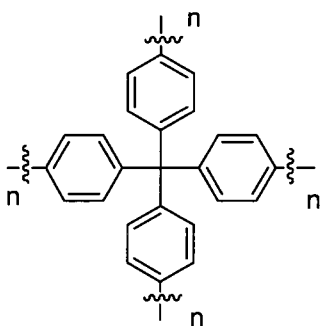
Reduced MOP. 104 mg of **Imine MOP**, in an oven dried flask was purged with $N_2(g)$ for 15 minutes. 15 mL of 1 M Borane-THF was then added to the flask and the mixture was allowed to stir for 24 hours at room temperature. The yellow solid was collected by filtration and washed with THF. **Reduced MOP** was collected in a 97 mg yield.



Amide MOP. 96 mg of **Reduced MOP** was submerged in Ac_2O for 18 hours to allow Ac_2O to exchange into the pores of the network. This mixture was then placed into a sealed glass tube and heated to 100 °C and stirred for 24 hours. The solid was collected via filtration, washed with THF and submerged in THF for 24 hours to allow any excess Ac_2O to exchange out of the network. The solid was again collected via filtration, washed with THF and collected, yielding 109 mg of **Amide MOP**.

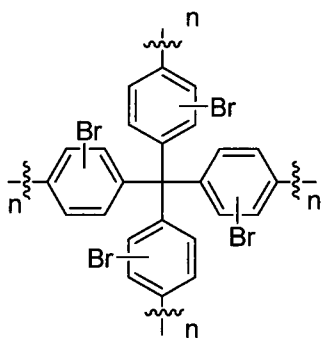


Tetrakis(4-bromophenyl)methane (12).⁸² Neat $\text{Br}_{2(l)}$ (6 ml, 117 mmol) was added dropwise to a flask charged with tetraphenylmethane **9** (3 g, 9.36 mmol) stirring slowly. The mixture was allowed to stir for 30 minutes and then diluted with 90 mL EtOH. The precipitate was filtered and washed with EtOH. A white powder was obtained (5.14 g, 87 %). ^1H NMR (300 MHz, CDCl_3) δ 7.39 (d, $J = 8.7$ Hz, 8H), δ 7.01 (d, $J = 8.4$ Hz, 8H); ^{13}C NMR (75 MHz, CDCl_3) δ 144.7, 132.5, 131.3, 121.0, 63.9; Elemental analysis calcd (%) for $\text{C}_{25}\text{H}_{16}\text{Br}_4$: C 47.21, H 2.54, Br 50.25; found: C 47.34, H 2.64, Br 50.00



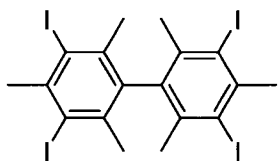
Tetraphenylmethane PAF.¹⁰ To an oven dried flask, purged with $\text{N}_{2(g)}$, within a nitrogen atmosphere glove box was added 2,2'-bipyridyl (0.32 g, 2.05 mmol), $\text{Ni}(\text{cod})_2$ (0.563 g, 2.05 mmol) and anhydrous DMF (30 mL). 1,5-cyclooctadiene (0.263 ml, 1.92 mmol) was then added from a Sureseal® bottle to the mixture resulting in a deep purple solution. The

solution was then heated at 80 °C for 1 hour at which point tetrakis(4-bromophenyl)methane **12** (0.25 g, 0.40 mmol) was added under a heavy flow of nitrogen. The resulting solution was then heated for 16 hours at 80 °C before cooling to room temperature. The resulting light grey precipitate was then filtered and washed with CHCl₃ (5x30 mL), H₂O (5x30 mL), THF (5x30 mL) and placed under vacuum heating at 100 °C for 12 hours. An off white solid was collected as **Tetraphenylmethane PAF** (0.121 g, 96 % yield assuming complete conversion). Elemental analysis calcd (%) for C₂₅H₁₆: C 94.94, H 5.06; found: C 85.56, H 5.37, Br 6.64.

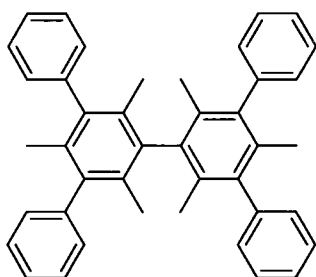


Brominated PAF. Neat Br_{2(l)} (8 mL, 117 mmol) was added dropwise to a flask charged with **tetraphenylmethane PAF** (50 mg) stirring slowly. The mixture was allowed to stir for 48 hours and then diluted with 50 mL DCM. The solid was filtered and washed thoroughly with DCM, suspended in DCM for 24 hours and filtered and washed with DCM again. The solid obtained was heated at 100 °C under vacuum in order to purge all guest molecules. An off white powder was obtained as **Brominated PAF** (83 mg).

Elemental analysis calcd (%) for $C_{25}H_{12}Br_4$: C 47.51, H 1.92, Br 50.57; found: C 44.39, H 2.09, Br 52.27.

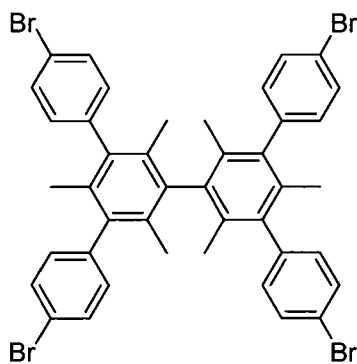


3,3',5,5'-tetraiodobimesityl (13).⁸⁵ To a mixture of AcOH (150 mL) and conc. H_2SO_4 (6 mL) was added bimesityl (2.0 g, 8.39 mmol), $I_{2(s)}$ (4.26 g, 16.77 mmol), and H_5IO_6 (1.91g, 8.39 mmol). The mixture was heated at 70 °C for 3 hours then cooled and poured over ice to form a pink precipitate. The precipitate was filtered and collected while the filtrate was extracted with $CHCl_3$, washed with 5 % sodium thiosulfate, dried over $MgSO_4$ and concentrated under reduced pressure to yield product. The original precipitate was redissolved in $CHCl_3$ and washed with 5 % sodium thiosulfate, dried over $MgSO_4$, filtered and concentrated under reduced pressure to also yield product. Total yield was 5.93 g (95 %). 1H NMR (300MHz, $CDCl_3$) δ 3.04 (s, 6H), δ 2.07 (s, 12H); ^{13}C NMR (75MHz, $CDCl_3$) δ 143.5, 139.38, 139.35, 105.5, 39.1, 28.2



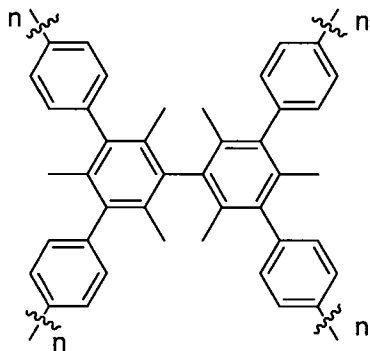
3,3',5,5'-tetraphenylbimesityl (14).⁸⁵ To an oven dried pressure tube cooled under $N_{2(g)}$ was added 3,3',5,5'-tetraiodobimesityl **13** (2.50 g, 3.37 mmol), phenylboronic acid (3.29

g, 26.96 mmol), and Pd(PPh₃)₄ (0.78 g, 0.67 mmol). The reaction tube was then purged with N_{2(g)} for 15 minutes while simultaneously degassing a toluene (18 mL)/ sat. NaHCO₃ (18 mL) solution. After degassing, the toluene/sat. NaHCO₃ was added to the reaction tube which was then sealed with a cap and o-ring. The reaction tube was heated from 80 °C to 120 °C under vigorous stirring and left at the latter temperature for 16 hours. The reaction tube was then cooled to room temperature and the impure product was extracted with CHCl₃, dried over MgSO₄, filtered and concentrated under reduced pressure. A column of 5 % CHCl₃ in hexanes yielded pure **14** (1.37 g, 75 %). ¹H NMR (300MHz, CDCl₃) δ 7.43 (t, J = 6.9Hz, 8H), δ 7.33 (t, J = 7.2Hz, 4H), δ 7.23 (d, J = 6.6Hz, 8H), δ 1.73 (s, 6H), δ 1.72 (s, 12H); ¹³C NMR (75MHz, CDCl₃) δ 142.5, 140.0, 138.7, 132.4, 131.9, 129.5, 126.2, 19.3, 18.3.



3,3',5,5'-tetra(4-bromophenyl)bimesityl (15).⁸⁵ Br_{2(l)} (0.20 mL, 3.87 mmol) was added dropwise to a solution of 3,3',5,5'-tetraphenylbimesityl **14** (0.50 g, 0.92 mmol) in the presence of Fe powder (0.05 g, 0.92 mmol) and allowed to stir at room temperature for 4 hours. The solution was then diluted with 50 mL of CHCl₃ and washed thoroughly with 2 M NaOH (5x50 mL). The organic layer was dried over MgSO₄, filtered and concentrated under reduced pressure to yield a white powder which was recrystallized in EtOAc

(0.74g, 94%). $^1\text{H NMR}$ (300MHz, CDCl_3): δ 7.54 (d, $J = 8.4\text{Hz}$, 8H), δ 7.07 (d, $J = 8.4\text{Hz}$, 8H), δ 1.67 (s, 6H), δ 1.64 (s, 12H); $^{13}\text{C NMR}$ (75MHz, CDCl_3) δ 140.9, 139.0, 138.5, 132.6, 132.0, 131.6, 131.2, 120.5, 19.3, 18.2; Elemental analysis calcd (%) for $\text{C}_{32}\text{H}_{24}\text{Br}_4$: C 58.77, H 3.99, Br 37.24; found: C 58.60, H 4.17, Br 37.29.



Bimesityl PAF. To an oven dried flask, purged with $\text{N}_2(\text{g})$, within a nitrogen atmosphere glove box was added 2,2'-bipyridyl (0.234 g, 1.5 mmol), $\text{Ni}(\text{cod})_2$ (0.413 g, 1.5 mmol) and anhydrous DMF (30 mL). 1,5-cyclooctadiene (0.172 ml, 1.4 mmol) was then added from a Sureseal® bottle to the mixture resulting in a deep purple solution. The solution was then heated at 80 °C for 1 hour at which point 3,3',5,5'-tetra(4-bromophenyl)bimesityl (0.25 g, 0.291 mmol) was added under a heavy flow of nitrogen. The resulting solution was then heated for 16 hours at 80 °C before cooling to room temperature. The resulting pale grey precipitate was then filtered and washed with CHCl_3 (5 x 30 mL), H_2O (5 x 30 mL), THF (5 x 30 mL) and place under vacuum heating at 100 °C for 12 h before being collected as **Bimesityl PAF** (0.121 g). Elemental analysis calcd (%) for $\text{C}_{32}\text{H}_{24}$: C 94.07, H 5.93; found: C 81.80, H 6.01, Br 7.58.

Chapter 7: References

- (1) Rouquerol J.; Avnir D.; Fairbridge C.W.; Everett D.H.; Haynes D.H.; Pernicone N.; Ramsay J.D.F.; Sing K.S.W.; Unger K.K. *Pure & Appl. Chem.*, **1994**, *66*, 1739.
- (2) Schuth F.; Sing K.S.W.; Weitkamp J. (eds). *Handbook of Porous Solids*, **2002**, Wiley, New York.
- (3) Maly K.E.; *J. Mater. Chem.* **2009**, *19*, 1781.
- (4) Davis M.E. *Nature*, **2002**, *417*, 813.
- (5) Morris R.E.; Wheatley P.S.; *Angew. Chem. Int. Ed.*, **2008**, *47*, 4966.
- (6) Côté A.P.; Benin A.I.; Ockwig N.W.; O’Keeffe M.; Matzger A.J.; Yaghi O.M. *Science*, **2005**, *310*, 1166.
- (7) El-Kaderi H.M.; Hunt J.R.; Mendoza-Cortes J.L.; Côté A.P.; Taylor R.E.; O’Keeffe M.; Yaghi O.M. *Science*, **2007**, *316*, 268.
- (8) Uribe-Romo F.J.; Hunt J.R.; Furukawa H.; Klock C.; O’Keeffe M.; Yaghi O.M. *J. Am. Chem. Soc.*, **2009**, *131*, 4570.
- (9) Jiang J.X.; Su F.; Trewin A.; Wood C.D.; Campbell N.L.; Niu H.; Dickinson C.; Ganin A.Y.; Rosseinsky M.J.; Khimyak Y.Z.; Cooper A.I. *Angew. Chem. Int. Ed. Engl.*, **2007**, *46*, 8574, see also correction, *Angew. Chem. Int. Ed. Engl.*, **2008**, *47*, 1167.
- (10) Ben T.; Ren H.; Ma S.; Cao D.; Lan J.; Jing X.; Wang W.; Xu J.; Deng F.; Simmons J.M.; Qiu S.; Zhu G. *Angew. Chem. Int. Ed. Engl.*, **2009**, *48*, 9457.
- (11) Eddaoudi M.; Moler, D.B.; Li H.; Chen B.; Reineke T.M.; O’Keeffe M.; Yaghi O.M. *Acc. Chem. Res.*, **2001**, *34*, 319.

- (12) Jiang J.X.; Cooper A.I. *Top Curr. Chem.* **2009**, 1.
- (13) Hoskins B.F.; Robson R. *J. Am. Chem. Soc.* **1990**, *112*, 1546.
- (14) Li H.; Davis C.; Richardson D.; Groy T.L.; Yaghi O.M. *Acc. Chem. Res.*, **1998**, *31*, 474.
- (15) Eddaoudi M.; Kim J.; Rosi N.; Vodak D.; Wachter J.; O’Keeffe M.; Yaghi O.M. *Science*, **2002**, *295*, 469.
- (16) A complete issue covering MOFs; *Chem. Soc. Rev.*, **2009**, *38*, 1201.
- (17) Wong-Foy A.G.; Matzger A.J.; Yaghi O.M. *J. Am. Chem. Soc.*, **2006**, *128*, 3494.
- (18) Lee C.H.; Filler R.; Lee J.Y.; Li J.; Mandal B.K. *Renewable Energy*, **2010**, *35*, 1592.
- (19) Bastin L.; Barcia P.S.; Hurtado E.J.; Silva J.A.C.; Rodrigues A.E.; Chen B.J. *J. Phys. Chem.*, **2008**, *112*, 1575.
- (20) Wu C.D.; Hu A.; Zhang L.; Lin W. *J. Am. Chem. Soc.* **2005**, *127*, 8940.
- (21) Kaye S.S.; Dailly A.; Yaghi O.M.; Long J.R. *J. Am. Chem. Soc.* **2007**, *129*, 14176.
- (22) Sabo M.; Henschel A.; Frode H.; Klemm E.; Kaskel S. *J. Mater. Chem.* **2007**, *17*, 3827.
- (23) Greathouse J.A.; Allendorf M.D. *J. Am. Chem. Soc.* **2006**, *128*, 10678.
- (24) Juan-Juan J.; Lozar-Marco J.P.; Suarez-Garcia F.; Cazorla-Amoros D.; Linares-Solano A. *Carbon*, **2010**, *48*, 2906.
- (25) McKeown N.B.; Makhseed S.; Budd P.M. *Chem. Commun.*, **2002**, 2780.
- (26) McKeown N.B.; Hanif S.; Msayib K.; Tattershall C.E.; Budd P.M. *Chem. Commun.*, **2002**, 2782.
- (27) Budd P.M.; Ghanem B.S.; Makhseed S.; McKeown N.B.; Msayib K.J.; Tattershall C.E. *Chem. Commun.*, **2004**, 230.

- (28) Budd P.M.; McKeown N.B.; Fritsch D. *J. Mater. Chem.*, **2005**, *15*, 1977.
- (29) Budd P.M.; Msayib K.J.; Tattershall C.E.; Ghanem B.S.; Reynolds K.J.; McKeown N.B.; Fritsch D. *J. Membrane Sci.*, **2005**, *251*, 263.
- (30) Ghanem B.S.; Msayib K.J.; McKeown N.B.; Harris K.D.M.; Pan Z.; Budd P.M.; Butler A.; Selbie J.; Book D.; Walton A. *Chem. Commun.*, **2007**, 67.
- (31) Weber J.; Su O.; Antonietti M.; Thomas A.; *Macromol. Rapid Commun.*, **2007**, *28*, 1871.
- (32) Li H.; Eddaoudi M.; O’Keeffe M.; Yaghi O.M. *Nature*, **1999**, *402*, 276.
- (33) Cheetham A.K.; Férey G.; Loiseau T. *Angew. Chem. Int. Ed. Engl.*, **1999**, *38*, 3268.
- (34) Yaghi O.M.; O’Keeffe M.; Ockwig N.W.; Chae H.K.; Eddaoudi M.; Kim J. *Nature*, **2003**, *423*, 705.
- (35) Kitagawa S.; Kitaura R.; Noro S. *Angew. Chem. Int. Ed. Engl.*, **2004**, *43*, 2334.
- (36) Hunt J.R.; Doonan C.J.; LeVangie J.D.; Côté A.P.; Yaghi O.M. *J. Am. Chem. Soc.* **2008**, *130*, 11872.
- (37) Banerjee R.; Phan A.; Wang B.; Knobler C.; Furukawa H.; O’Keeffe M.; Yaghi O.M. *Science*, **2008**, *319*, 939.
- (38) Wang B.; Côté A.P.; Furukawa H.; O’Keeffe M.; Yaghi O.M. *Nature*, **2008**, *453*, 207.
- (39) James S.L. *Chem. Soc. Rev.*, **2003**, *32*, 276.
- (40) Janiak C. *Dalton Trans.*, **2003**, 2781.
- (41) Kitagawa S.; Kitaura R.; Noro S. *Angew. Chem., Int. Ed.*, **2004**, *43*, 2334.
- (42) Chong J.H.; MacLachlan M.J. *Inorg. Chem.*, **2006**, *45*, 1442.
- (43) Furukawa H.; Yaghi O.M. *J. Am. Chem. Soc.*, **2009**, *131*, 8875.

- (44) Davankov V.A.; Tsyurupa M.P. *React. Polym.*, **1990**, *13*, 27.
- (45) Budd P.M.; Ghanem B.S.; Makhseed S.; McKeown N.B.; Msayib K.J.; Tattershall C.E. *Chem. Commun.*, **2004**, 230.
- (46) Weber J.; Su O.; Antonietti M.; Thomas A.; *Macromol. Rapid Commun.*, **2007**, *28*, 1871.
- (47) Jiang J.X.; Su F.; Niu H.; Wood C.D.; Campbell N.L.; Khimyak Y.Z.; Cooper A.I. *Chem. Commun.*, **2008**, 486.
- (48) Kuhn P.; Antonietti M.; Thomas A. *Angew. Chem. Int. Ed. Engl.*, **2008**, *47*, 3450.
- (49) Wang Z.; Cohen M. *Chem. Soc. Rev.*, **2009**, *38*, 1315.
- (50) Wang Z.; Cohen S.M. *J. Am. Chem. Soc.*, **2007**, *129*, 12368.
- (51) Kawamichi T.; Kodama T.; Kawano M.; Fujita M. *Angew. Chem., Int. Ed.*, **2008**, *47*, 8030.
- (52) Wang Z.; Tanabe K.K.; Cohen S.M.; *Inorg. Chem.*, **2009**, *48*, 296.
- (53) Burrows A.D.; Frost C.G.; Mahon M.F.; Richardson C. *Angew. Chem., Int. Ed.*, **2008**, *47*, 8482.
- (54) Haneda T.; Kawano M.; Kawamichi T.; Fujita M. *J. Am. Chem. Soc.*, **2008**, *130*, 1578.
- (55) Kawamichi T.; Kodama T.; Kawano M.; Fujita M. *Angew. Chem., Int. Ed.*, **2008**, *47*, 8030.
- (56) Seo J.S.; Whang D.; Lee H.; Jun S.I.; Oh J.; Jeon Y.J.; Kim K. *Nature*, **2000**, *404*, 982.
- (57) Wang Z.; Cohen S.M. *Angew. Chem., Int. Ed.*, **2008**, *47*, 4699.

- (58) Morris W.; Doonan C.J.; Furukawa H.; Banerjee R.; Yaghi O.M. *J. Am. Chem. Soc.*, **2008**, *130*, 12626.
- (59) Wang X.S.; Ma S.; Sun D.; Parkin S.; Zhou H.C. *J. Am. Chem. Soc.*, **2006**, *128*, 16474.
- (60) Tanabe K.K.; Wang Z.; Cohen S.M.; *J. Am. Chem. Soc.*, **2008**, *130*, 8508.
- (61) Niyogi S.; Hamon M.A.; Zhao H.H.B.; Bhowmik P.; Sen R.; Itkis M.E.; Haddon R.C. *Acc. Chem. Res.*, **2002**, *35*, 1105.
- (62) Hirsch A. *Angew. Chem., Int. Ed.*, **2002**, *41*, 1853.
- (63) Banerjee S.; Kahn M.G.C.; Wong S.S. *Chem.–Eur. J.*, **2003**, *9*, 1899.
- (64) Tasis D.; Tagmatarchis N.; Bianco A.; Prato M. *Chem. Rev.*, **2006**, *106*, 1105.
- (65) Sun Y.P.; Fu K.; Lin Y.; Huang W. *Acc. Chem. Res.*, **2002**, *35*, 1096.
- (66) Hoffmann F.; Cornelius M.; Morell J.; Froba M. *Angew. Chem., Int. Ed.*, **2006**, *45*, 3216.
- (67) Bartlett P. D.; Ryan M. J.; Cohen S.G. *J. Am. Chem. Soc.*, **1942**, *64*, 2649.
- (68) Hart H.; Shamouilian S.; Takehira Y. *J. Org. Chem.*, **1981**, *46*, 4427.
- (69) Chong J. H.; MacLachlan M. J. *Chem. Soc. Rev.*, **2009**, *38*, 3301.
- (70) Tsui N.T.; Torun L.; Pate B.D.; Paraskos A.J.; Swager T.M.; Thomas E.L. *Adv. Funct. Mater.*, **2007**, *17*, 1595.
- (71) Klanderman B.H.; Faber J.W.H. *J. Polym. Sci., Polym. Chem. Ed.*, **1968**, *6*, 2955.
- (72) Hoffmeister E.; Kropp J.E.; McDowell T.L.; Michel R.H.; Rippie W.L. *J. Polym. Sci., Polym. Chem. Ed.*, **1969**, *7*, 55.
- (73) Yang J.S.; Swager T.M. *J. Am. Chem. Soc.*, **1998**, *120*, 5321.
- (74) Zhao D.; Swager T.M. *Org. Lett.*, **2005**, *7*, 4357.

- (75) Zhao D.; Swager T.M. *Macromolecules*, **2005**, *38*, 9377.
- (76) Chong J. H.; MacLachlan M. J., *Inorg. Chem.*, **2006**, *45*, 1442.
- (77) Shklyayev Y.V.; Nifontov Y.V. *Russ. Chem. Bull. Int. Ed.*, **2002**, *51*, 844.
- (78) Zhu X.Z.; Chen C.F. *J. Am. Chem. Soc.*, **2005**, *127*, 13158.
- (79) Li Y. ; Yang R.T. *AIChE J.*, **2008**, *54*, 269.
- (80) Katritzky A.R.; Yao G. ; Lan X. ; Zhao X. *J. Org. Chem.*, **1993**, *58*, 2086.
- (81) National Institute of Advanced Industrial Science and Technology (AIST), Japan.
Spectral Database for Organic Compounds, http://riodb01.ibase.aist.go.jp/sdbs/cgi-bin/cre_index.cgi?lang=eng.
- (82) Plietzsch O.; Schilling C.I.; Tolev M.; Nieger M.; Richert C.; Bräse T.M.S. *Org. Biomol. Chem.*, **2009**, *7*, 4734.
- (83) Kiemle D.J.; Silverdtein R.M.; Webster F.X. *Spectrometric Identification of Organic Compounds, Seventh Ed.*, **2005**, Wiley, New Jersey.
- (84) Fischer E.; Hess H.; Lorenz T.; Musso H.; Rossnagel I. *Chem. Ber.*, **1991**, *124*(4), 783.
- (85) Moorthy J.N.; Venkatakrishnan P.; Natarajan P.; Huang D.F.; Chow T.J. *J. Am. Chem. Soc.*, **2008**, *130*, 17320.